AIMS Mathematics, 11(9): 30782–30814.
DOI:10.3934/math.20261219
Received: 27 February 2026
Revised: 31 August 2026
Accepted: 08 September 2026
Published: 21 September 2026

https://www.aimspress.com/journal/Math

Theory article

Tumor–immune dynamics: stability, optimal control, and global sensitivity analysis

Nacima Moussouni[1,2], Louiza Dehbi[3], Fares Yazid[3], Hicham Saber[4], Abdelkader Moumen[4,*], Khaled Aldwoah[5] and Mohamed Bouye[6]

[1] Faculty of Medicine, Amar Telidji University of Laghouat, 03000 Laghouat, Algeria

[2] L2CSP Laboratory, Mouloud Mammeri University of Tizi-Ouzou, Hasnaoua II Campus, P.O. Box 17 RP, 15000, Tizi-Ouzou, Algeria

[3] Laboratory of Pure and Applied Mathematics, Amar Telidji University of Laghouat, P.O. Box 37 G, 03000 Laghouat, Algeria

[4] Department of Mathematics, College of Science, University of Ha'il, 55473 Ha'il, Saudi Arabia

[5] Department of Mathematics, Faculty of Science, Islamic University of Madinah, Madinah 42351, Saudi Arabia

[6] Department of Mathematics, Faculty of Sciences, King Khalid University, P.O. Box 9004, Abha, Saudi Arabia

* **Correspondence:** Email: mo.abdelkader@uoh.edu.sa.

Abstract: Oncology is one of the most important fields in modern medicine. In this work, we aimed to model tumor–immune interactions using a system of ordinary differential equations. Our objective of this modeling was to help control tumor cell growth (with a carrying capacity that is a function of time) in the human body while determining an optimal treatment strategy. To achieve this goal, we first introduced our model and studied its main characteristics. We then investigated the existence and uniqueness of solutions. Afterward, we analyzed the stability of the system. Next, we addressed the optimal control problem theoretically using Pontryagin's Maximum Principle and, numerically using direct and indirect methods, implemented it in MATLAB. We also performed numerical simulations corresponding to different treatment scenarios. Finally, we studied the sensitivity of the model parameters by means of Partial Rank Correlation Coefficients (PRCC) to identify the most influential ones.

Keywords: tumor–immune cells; Pontryagin's Maximum Principle; partial rank correlation coefficient (PRCC); Rosenzweig–MacArthur model
Mathematics Subject Classification: 92C50, 93C10

1. Introduction

Oncology is the branch of medicine devoted to the study, diagnosis, treatment, and prevention of cancer. It focuses on tumor cells and their interactions with the components of the human body and investigates different therapeutic approaches for various types of cancer. For a comprehensive understanding of this field, readers may refer to the fundamental textbooks [1] and [2].

To study these phenomena from a mathematical perspective, researchers have proposed mathematical models formulated using differential equations. Among the pioneering works, we may cite P. Essunger and A. S. Perelson [3], who investigated the interactions between tumor-like infected cells and the immune system by modeling HIV interactions with $CD4^+$ T-cell subpopulations. Their work demonstrated that the virus depletes memory T-cells as well as peripheral and thymic T-cell precursors, while resting cells become fully infected only after activation. A few years later, H. Moore and coauthors [4] proposed and analyzed a mathematical model for chronic myelogenous leukemia (CML) describing the interactions between naive T-cells, effector T-cells, and leukemic cells. Their analysis identified the tumor growth and death rates as the most critical parameters for remission, suggesting that treatments targeting these rates may be particularly effective.

Moreover, contributions include [5], where the authors investigated cancer treatment strategies using chemotherapy and immunotherapy, both individually and in combination. In [6], the authors modeled tumor growth under chemotherapy and analyzed the dynamical behavior of the corresponding solutions; however, unlike our proposed model, they assumed a constant carrying capacity.

These models are often inspired by predator–prey frameworks, in which tumor cells are viewed as the prey and immune effector cells as the predators. Such models may be formulated using ordinary differential equations, partial differential equations, stochastic differential equations, or other types of mathematical frameworks. In this work, we focus on ordinary differential equations, for which three principal models can be identified:

- **Lotka–Volterra model**, where it is assumed that the prey increase exponentially and the predator-prey interaction is linear. It was first introduced independently by Lotka in 1925 [7] and Volterra in 1926 [8]; together, they proposed the following model:

$$\begin{cases} \frac{dx}{dt} = \alpha x - \beta xy, \\ \frac{dy}{dt} = \delta xy - \gamma y. \end{cases}$$

  Several studies have been conducted based on this model; for instance, we may refer to [9, 10]. Subsequently, this model was extended to include logistic prey growth, leading to the following system:

$$\begin{cases} \frac{dx}{dt} = rx\left(1 - \frac{x}{K}\right) - f(x)y. \\ \frac{dy}{dt} = g(x)y - dy, \end{cases}$$

  This model represents a combination of the Lotka–Volterra system and the Verhulst logistic equation, which was introduced in 1838 by P. F. Verhulst. Models of this type can be found in studies such as [11, 12].

- **Holling model:** Holling introduced three different models describing the predator's functional response.

-Holling Type I: It describes a linear increase in the form of $f(N) = aN$.
-Holling Type II ([13, 14]): This is the model of interest in this study. It describes a saturating response of the form

$$f(N) = \frac{aN}{1 + ahN}.$$

-Holling Type III ([15, 16]): It describes a sigmoidal response of the form

$$f(N) = \frac{aN^2}{1 + ahN^2}.$$

- **Rosenzweig–MacArthur model:** This model was first introduced by MacArthur and Rosenzweig in 1963. It combines logistic prey growth with a Holling type II functional response and is given by

$$\begin{cases} \frac{dx}{dt} = rx(1 - \frac{x}{k}) - \frac{ax}{1+ahx}y, \\ \frac{dy}{dt} = b\frac{ax}{1+ahx}y - my, \end{cases}$$

Several works have studied this model; as an example, we can cite [17].

The theory of optimal control began in the 1950s, when Pontryagin and his collaborators introduced a theoretical framework for solving optimal control problems, known as Pontryagin's Maximum Principle. A comprehensive summary of his selected works can be found in [18]. Subsequently, in the 1960s and 1970s, linear quadratic control was developed by several researchers, including R. Kalman and Bryson. Moreover, optimal control theory has been extended to nonlinear systems and to problems with more complex state and control constraints.

In [19], the authors studied the optimal control of interactions among whiteflies, citrus fruits, and birds using a predator–prey model. Additional contributions in this field include [20], who focused on optimizing cancer treatment using optimal control theory but did not address the influence of a variable carrying capacity on treatment optimization. Similarly, in [21], the authors formulated an optimal control problem to eradicate tumor cells by analyzing interactions among effector, tumor, and normal cells under immunotherapy treatment.

Global sensitivity analysis is widely employed in applied mathematics to identify the parameters that most significantly influence the overall dynamics of a system (see, e.g., [22, 23]). In this work, it is carried out by means of *Partial Rank Correlation Coefficients* (PRCC), a rank-based statistical index that measures the monotone association between each input parameter and a scalar model output while controlling for the effect of all remaining parameters. The acronym PRCC is used with this meaning throughout the paper.

In our work, we consider a cancer model based on the Rosenzweig–MacArthur framework. While other researchers have investigated similar models with a constant carrying capacity, we extend this framework by treating the tumor carrying capacity as a time-dependent state variable.

Motivation for a time-dependent carrying capacity. In the classical logistic and Rosenzweig–MacArthur formulations, the carrying capacity $\mathcal{K}$ is a fixed constant, which implicitly assumes that the resources available to the tumor are set once and for all. This assumption is biologically unrealistic for solid tumors. A tumor larger than roughly 1–2 mm^3 can no longer be sustained by passive diffusion alone and must recruit its own vascular network through angiogenesis. The nutrient supply, and hence the maximal tumor burden that the micro-environment can sustain, is therefore not a constant but a

dynamic variable driven by the tumor and degraded by natural vessel regression and by anti-angiogenic action. This is precisely what the fourth equation of our model encodes: The term $\lambda\mathcal{T}$ represents neo-vascularization induced by the tumor (the carrying capacity grows in proportion to the tumor that recruits it), while $-\delta\mathcal{K}$ represents the spontaneous decay and therapy-induced regression of that vasculature. This equation is the linearized form of the vascular-support model of Hahnfeldt et al. [24], which was calibrated on Lewis lung carcinoma data. Treating $\mathcal{K}$ as a state variable rather than a parameter thus converts an exogenous constant into an endogenous, therapeutically addressable target, and it is what enables anti-angiogenic strategies (acting on λ and δ) to be compared with cytotoxic strategies (acting on $K_{\mathcal{T}}$) within a single framework. Compared with a constant-capacity model, this formulation reproduces the clinically observed phenomenon that reducing the vascular support of a tumor lowers its sustainable size even when the tumor proliferation rate r is unchanged.

Research gap. The models discussed above address either tumor–immune interactions with a constant carrying capacity, or optimal therapy scheduling, or parameter sensitivity, but rarely all three together. Specifically: (i) The Rosenzweig–MacArthur-type tumor models of [12, 17] retain a constant capacity and do not include therapy; (ii) the control-oriented studies [20, 21] incorporate treatment but keep the environmental capacity fixed, so that anti-angiogenic action cannot be represented; and (iii) sensitivity studies such as [22, 23] are carried out on models without an optimal-control layer. To the best of our knowledge, no previous contribution combines a tumor–immune system with an explicitly dynamic, tumor-driven carrying capacity, a rigorous qualitative analysis (positivity, boundedness, existence and stability), a Pontryagin-based optimal control formulation solved by both direct and indirect methods, and a global PRCC sensitivity analysis. Here, we address this gap.

The main contributions of this work can be summarized as follows:

- A tumor-immune model with time-dependent carrying capacity is proposed.
- The existence, positivity, and boundedness of solutions are established.
- The stability of equilibrium points is analyzed.
- An optimal control problem is formulated and solved.
- A global sensitivity analysis based on partial rank correlation coefficients (PRCCs) is performed.

The paper is organized as follows: In Section 2, we develop the mathematical formulation of the problem using a predator–prey system. In Section 3, we investigate fundamental properties of the system, including positivity and boundedness. In Section 4, we address the existence and uniqueness of solutions using the Cauchy–Lipschitz theorem. In Section 5, we analyze the asymptotic behavior of solutions near equilibrium points via the Jacobian method, illustrated with numerical simulations. In Section 6, we introduce the objective functional, which depends on the control V_m, representing the external treatment administration rate; this problem is studied theoretically using Pontryagin's Maximum Principle and numerically through several methods implemented in MATLAB. Various scenarios are considered, including treatment interruption, comparison of therapies, and combination strategies. Section 7 is devoted to parameter sensitivity analysis based on the computation of partial rank correlation coefficients (PRCCs) and their associated p-values. Finally, the main results are summarized in a concise conclusion.

2. Statement of the problem

In our work, we focus on the study of immuno-effector cells ($\mathcal{E}$), tumor cells ($\mathcal{T}$), treatment ($\mathcal{M}$), and carrying capacity ($\mathcal{K}$), which are defined by the following ODE system:

$$\begin{cases} \frac{d\mathcal{E}}{dt} = s - \mu\mathcal{E} + p\frac{\mathcal{E}\mathcal{T}}{h+\mathcal{T}} - m\mathcal{E}\mathcal{T} - K_{\mathcal{E}}\mathcal{M}\mathcal{E}, \\ \frac{d\mathcal{T}}{dt} = r\mathcal{T}\left(1 - \frac{\mathcal{T}}{\mathcal{K}}\right) - a\frac{\mathcal{E}\mathcal{T}}{g+\mathcal{T}} - K_{\mathcal{T}}\mathcal{M}\mathcal{T}, \\ \frac{d\mathcal{M}}{dt} = -\gamma\mathcal{M} + V_m, \\ \frac{d\mathcal{K}}{dt} = \lambda\mathcal{T} - \delta\mathcal{K}, \end{cases} \tag{2.1}$$

The last equation reflects the temporal evolution of the tumor microenvironment as the disease progresses. As the tumor grows, it alters its surrounding environment, thereby increasing the maximum tumor population that the tissue can sustain.
Where

p	The degree of recruitment of maximum immune-effector cells in relation to cancer cells.
r	The rate of tumor growth.
a	The parameter of cancer clean-up.
s	The natural growth rate of normal/effector cells.
m	The degree of inactivation of effector cells by tumor cells.
μ	The rate of natural demise of effector cells.
γ	The rate of decrease in concentration of chemotherapy drug.
h	The steepness coefficient of the recruitment curve of effector immune cells.
g	The half-saturation constant for cancer cleanup.
V_m	The volume of the medicine that had been administered from outside the body.
$K_{\mathcal{E}}$	The drug-induced loss (kill) rate of effector cells.
$K_{\mathcal{T}}$	The drug-induced kill rate of tumor cells.
δ	The natural decay (regression) rate of the carrying capacity.
λ	The speed of tumor vascularization.

Remark 1. *Parameters $K_{\mathcal{E}}$ and $K_{\mathcal{T}}$ multiply the terms $-K_{\mathcal{E}}\mathcal{M}\mathcal{E}$ and $-K_{\mathcal{T}}\mathcal{M}\mathcal{T}$, respectively; they therefore quantify the* destruction *of effector and tumor cells caused by the cytotoxic agent, and not their appearance. The corresponding entries of the parameter list have been corrected accordingly, and are consistent with the signs obtained in the sensitivity analysis of Section 7.*

The initial conditions are

$$\mathcal{E}(0) = \mathcal{E}_0 \geq 0, \;\; \mathcal{T}(0) = \mathcal{T}_0 \geq 0, \;\; \mathcal{M}(0) = \mathcal{M}_0 \geq 0, \;\; \mathcal{K}(0) = \mathcal{K}_0 > 0.$$

The strict inequality $\mathcal{K}_0 > 0$ is required because $\mathcal{K}$ appears in the denominator of the second equation of (2.1); the vector field is not defined for $\mathcal{K} = 0$. Lemma 1 below shows that this strict positivity propagates for all $t \geq 0$, so that system (2.1) is well posed on the whole interval considered.

3. Positivity and boundedness

In this section, we examine whether the solutions of model (2.1) are meaningful. To do this, we will establish the following lemmas.

Lemma 1. *Let $\mathcal{E}_0, \mathcal{T}_0, \mathcal{M}_0 \geq 0$ and $\mathcal{K}_0 > 0$. Then the corresponding solution of system* (2.1) *satisfies $\mathcal{E}(t) \geq 0$, $\mathcal{T}(t) \geq 0$, $\mathcal{M}(t) \geq 0$ and $\mathcal{K}(t) > 0$ for all $t \geq 0$ in the maximal interval of existence.*

Proof. We treat the four states separately. Throughout, $[0, T_f]$ denotes a compact subinterval of the maximal interval of existence.

- For the state $\mathcal{T}$:

From the second equation of system (2.1), $\mathcal{T}$ satisfies the linear (in $\mathcal{T}$) equation

$$\frac{d\mathcal{T}}{dt} = \mathcal{T}\left(r\left(1 - \frac{\mathcal{T}}{\mathcal{K}}\right) - a\frac{\mathcal{E}}{g + \mathcal{T}} - K_{\mathcal{T}}\mathcal{M}\right),$$

whose solution can be written in the multiplicative form

$$\mathcal{T}(t) = \mathcal{T}_0 \exp\left(\int_0^t \left[r\left(1 - \frac{\mathcal{T}(\tau)}{\mathcal{K}(\tau)}\right) - a\frac{\mathcal{E}(\tau)}{g + \mathcal{T}(\tau)} - K_{\mathcal{T}}\mathcal{M}(\tau)\right] d\tau\right) \geq 0.$$

Since the exponential is strictly positive, $\mathcal{T}(t) \geq 0$ for all t, and $\mathcal{T}(t) > 0$ whenever $\mathcal{T}_0 > 0$.

- For the state $\mathcal{M}$: We have, for all $t \in [0, T_f]$,

$$\mathcal{M}(t) = \mathcal{M}_0\, e^{-\gamma t} + \frac{V_m}{\gamma}(1 - e^{-\gamma t}) \geq 0.$$

- For the state $\mathcal{K}$ (strict positivity), solving the fourth equation by the variation-of-constants formula and using $\mathcal{T} \geq 0$ established above,

$$\mathcal{K}(t) = \mathcal{K}_0\, e^{-\delta t} + \lambda \int_0^t e^{-\delta(t-\tau)}\mathcal{T}(\tau)\, d\tau \;\geq\; \mathcal{K}_0\, e^{-\delta t} \;>\; 0,$$

because $\mathcal{K}_0 > 0$ and the integral term is non-negative. Hence, $\mathcal{K}$ never vanishes on $[0, T_f]$, the quotient $\mathcal{T}/\mathcal{K}$ in (2.1) is well defined, and the second equation of (2.1) is non-singular. This justifies rigorously the strict inequality imposed on $\mathcal{K}_0$ in Section 2.

- For the state $\mathcal{E}$, we argue by contradiction, taking care to work at the first time at which $\mathcal{E}$ reaches zero, which is the point at which the sign information is actually available. Suppose that $\mathcal{E}$ becomes negative and set

$$t_0 := \inf\{t \in [0, T_f] :\ \mathcal{E}(t) < 0\}.$$

By continuity of $\mathcal{E}$ and since $\mathcal{E}_0 \geq 0$, we have $\mathcal{E}(t_0) = 0$ and $\mathcal{E}(t) \geq 0$ for all $t \in [0, t_0]$. Evaluating the first equation of (2.1) at $t = t_0$ and using $\mathcal{E}(t_0) = 0$, every term containing the factor $\mathcal{E}$ vanishes, so that

$$\frac{d\mathcal{E}}{dt}(t_0) = s - \mu \cdot 0 + p\frac{0 \cdot \mathcal{T}(t_0)}{h + \mathcal{T}(t_0)} - m \cdot 0 \cdot \mathcal{T}(t_0) - K_{\mathcal{E}}\mathcal{M}(t_0) \cdot 0 = s > 0.$$

Therefore, $\mathcal{E}$ is strictly increasing in a neighborhood of t_0, which contradicts the definition of t_0 as the infimum of the times at which $\mathcal{E}$ becomes negative. Consequently $\mathcal{E}(t) \geq 0$ for all $t \in [0, T_f]$. □

Remark 2. *The previous argument makes explicit the point at which the equality $\mathcal{E}(t_0) = 0$ is used. This equality is not an additional assumption: It is a consequence of the definition of t_0 as the first time at which $\mathcal{E}$ vanishes, together with the continuity of $\mathcal{E}$ and the non-negativity of $\mathcal{E}_0$. It is precisely at such a point, and only there, that the first equation of* (2.1) *reduces to $d\mathcal{E}/dt = s > 0$.*

Lemma 2. *Consider the following assumptions:*
$(H1) : \mu > p.$
$(H2) : \lambda < \delta.$
Under these two assumptions each solution of system (2.1) *is bounded.*

Remark 3. *Assumption* (*H*2)*, namely $\lambda < \delta$, is biologically meaningful: If it fails, the tumor-driven neo-vascularization outpaces vascular regression, the carrying capacity grows without bound, and the tumor cells may blow up in finite time.*

Proof. We first bound $\mathcal{K}$, then $\mathcal{T}$, then $\mathcal{M}$ and $\mathcal{E}$.

Total-mass estimate. Define $W(t) := \mathcal{T}(t) + \dfrac{r}{\lambda}\mathcal{K}(t) \geq 0$. Differentiating and using (2.1) with $\mathcal{E}, \mathcal{M} \geq 0$ and $\mathcal{K} > 0$ (Lemma 1),

$$\frac{dW}{dt} = r\mathcal{T} - \frac{r\mathcal{T}^2}{\mathcal{K}} - a\frac{\mathcal{E}\mathcal{T}}{g+\mathcal{T}} - K_{\mathcal{T}}\mathcal{M}\mathcal{T} + \frac{r}{\lambda}(\lambda\mathcal{T} - \delta\mathcal{K}) \leq r\mathcal{T} - \frac{r\mathcal{T}^2}{\mathcal{K}} + r\mathcal{T} - \frac{r\delta}{\lambda}\mathcal{K}.$$

Using the elementary inequality $2\mathcal{T} \leq \dfrac{\mathcal{T}^2}{\mathcal{K}} + \mathcal{K}$, which is valid for every $\mathcal{K} > 0$ since it is equivalent to $0 \leq (\mathcal{T} - \mathcal{K})^2/\mathcal{K}$, we obtain

$$\frac{dW}{dt} \leq r\mathcal{K} - \frac{r\delta}{\lambda}\mathcal{K} = r\mathcal{K}\left(1 - \frac{\delta}{\lambda}\right).$$

Under $(H2)$, $\delta/\lambda > 1$, hence $1 - \delta/\lambda < 0$ and therefore $\frac{dW}{dt} \leq -\eta\mathcal{K}$ with $\eta := r\left(\frac{\delta}{\lambda} - 1\right) > 0$. In particular W is non-increasing, so

$$\mathcal{T}(t) \leq W(t) \leq W(0) = \mathcal{T}_0 + \frac{r}{\lambda}\mathcal{K}_0 =: \alpha_2 \qquad \text{for all } t \geq 0,$$

and consequently $\mathcal{K}(t) \leq \frac{\lambda}{r}W(0) =: \alpha_4$. $\mathcal{T}$ and $\mathcal{K}$ are thus globally bounded, which is the assertion required in the sequel.

Bound on $\mathcal{M}$. From the third equation,

$$\mathcal{M}(t) = \mathcal{M}_0\, e^{-\gamma t} + \frac{V_m}{\gamma}(1 - e^{-\gamma t}), \quad t \geq 0,$$

then

$$\limsup_{t\to+\infty} \mathcal{M}(t) \leq \alpha_3.$$

With $\alpha_3 = \max\left\{M_0, \frac{V_m}{\gamma}\right\}$

Bound on $\mathcal{E}$. Using the first equation and $\frac{\mathcal{T}}{h+\mathcal{T}} < 1$,

$$\frac{d\mathcal{E}}{dt} \leq s + (p - \mu)\mathcal{E},$$

so, since $(H1)$ gives $\mu - p > 0$,

$$\mathcal{E}(t) \leq \mathcal{E}_0\, e^{-(\mu-p)t} + \frac{s}{\mu - p}\left(1 - e^{-(\mu-p)t}\right), \quad t \geq 0.$$

Hence, by assumption $(H1)$,

$$\limsup_{t\to+\infty} \mathcal{E}(t) \leq \alpha_1.$$

Where $\alpha_1 := \max\left\{E_0, \frac{s}{\mu-p}\right\}$
All four states are therefore bounded, which completes the proof. □

Remark 4. *The assumption $\lambda < \delta$ is biologically reasonable because it implies that the loss rate of the carrying capacity exceeds its tumor–induced production rate, thereby preventing an excessive accumulation of carrying capacity.*

4. Existence and uniqueness

In this section, we study the existence and uniqueness of solutions to our problem. We state the following theorem:

Theorem 1. *Under the assumptions $(H1) - (H2)$, system (2.1) admits a unique solution.*

Proof. Let us define function $\mathcal{F}(X)$ by

$$\mathcal{F}(X) = \begin{pmatrix} \mathcal{F}_1(X) \\ \mathcal{F}_2(X) \\ \mathcal{F}_3(X) \\ \mathcal{F}_4(X) \end{pmatrix} = \begin{pmatrix} s - \mu\mathcal{E} + p\frac{\mathcal{E}\mathcal{T}}{h+\mathcal{T}} - m\mathcal{E}\mathcal{T} - K_{\mathcal{E}}\mathcal{M}\mathcal{E} \\ r\mathcal{T}\left(1 - \frac{\mathcal{T}}{\mathcal{K}}\right) - a\frac{\mathcal{E}\mathcal{T}}{g+\mathcal{T}} - K_{\mathcal{T}}\mathcal{M}\mathcal{T} \\ -\gamma\mathcal{M} + V_m \\ \lambda\mathcal{T} - \delta\mathcal{K} \end{pmatrix}, \tag{4.1}$$

where $X = \begin{pmatrix} \mathcal{E} \\ \mathcal{T} \\ \mathcal{M} \\ \mathcal{K} \end{pmatrix}$.

To prove the existence and uniqueness of the solution, we show that the function (4.1) is Lipschitz continuous.

Let $X = \begin{pmatrix} \mathcal{E} \\ \mathcal{T} \\ \mathcal{M} \\ \mathcal{K} \end{pmatrix}$ and $X' = \begin{pmatrix} \mathcal{E}' \\ \mathcal{T}' \\ \mathcal{M}' \\ \mathcal{K}' \end{pmatrix}$

By positivity and boundedness of the system stated previously, any solution starting from $\mathcal{E}_0, \mathcal{T}_0, \mathcal{M}_0, \mathcal{K}_0$ remains, for all $t \in [0, T_f]$, in the compact convex set

$$\Omega = [0, \alpha_1] \times [0, \alpha_2] \times [0, \alpha_3] \times [k_{\min}, \alpha_4],$$

where $\alpha_1, \alpha_2, \alpha_3, \alpha_4$ are the bounds of our functions, and $k_{\min} := \mathcal{K}_0 e^{-\delta T_f} > 0$ follows from $\dot{\mathcal{K}} = \lambda\mathcal{T} - \delta\mathcal{K} \geq -\delta K$.

On Ω, all denominators ($h + \mathcal{T} \geq h$, $g + \mathcal{T} \geq g$, $\mathcal{K} \geq k_{\min}$) are bounded away from zero; hence, $\mathcal{F} \in C^1(\Omega)$. Since Ω is compact, by the Weierstrass theorem, each entry of the Jacobian $D\mathcal{F}$ is bounded on Ω ; in particular $|\partial\mathcal{F}_2/\partial\mathcal{K}| = r\mathcal{T}^2/\mathcal{K}^2 \leq r\alpha_2^2/k_{\min}^2 < \infty$, so the term that was singular at $\mathcal{K} = 0$ is therefore controlled. Since Ω is convex, the mean value inequality yields, for all $X, X' \in \Omega$,

$$\|\mathcal{F}(X) - \mathcal{F}(X')\|_1 \leq L\|X - X'\|_1, \qquad L := \sup_{X\in\Omega} \|D\mathcal{F}(X)\|_1 < \infty,$$

so $\mathcal{F}$ is Lipschitz continuous on Ω.

By the Cauchy-Lipschitz theorem, system (2.1) admits a unique local solution. Since this solution remains in the compact set Ω, it cannot blow up in finite time. We then conclude the existence and uniqueness of a global solution. □

5. Stability analysis

5.1. Local stability

To study local stability, we determine the equilibrium points of system (2.1), which satisfy

$$\frac{d\mathcal{E}}{dt} = \frac{d\mathcal{T}}{dt} = \frac{d\mathcal{M}}{dt} = \frac{d\mathcal{K}}{dt} = 0.$$

We distinguish three cases:

1) If $\mathcal{E} = \mathcal{T} = 0$, the equilibrium point of system (2.1) is $E_0(0, 0, \frac{V_m}{\gamma}, 0)$.

   Remark 5. *This case is called a trivial equilibrium point, meaning that neither immunity nor tumors is present. This situation is biologically almost impossible.*

2) If $\mathcal{T} = 0$, the equilibrium point of system (2.1) is $E_1(\frac{s}{\mu + K_E\frac{V_m}{\gamma}}, 0, \frac{V_m}{\gamma}, 0)$.

   Remark 6. *This case is referred to as the disease-free equilibrium point, which corresponds to the absence of tumor cells. This corresponds to a strong immune response.*

3) $\mathcal{E} \neq 0$ and $\mathcal{T} \neq 0$, we obtain the following equilibrium points

   $$\mathcal{E}^* = \frac{s}{\mu - p\frac{\mathcal{T}^*}{h+\mathcal{T}^*} + m\mathcal{T}^* + K_{\mathcal{E}}\frac{V_m}{\gamma}}, \mathcal{T}^* = -g + \frac{a\mathcal{E}^*}{r(1 - \frac{\delta}{\lambda}) - K_{\mathcal{T}}\frac{V_m}{\gamma}},$$

   $\mathcal{M}^* = \frac{V_m}{\gamma}$ and $\mathcal{K}^* = \frac{\lambda}{\delta}\mathcal{T}^*$.

   Hence,

   $$(\mathcal{E}^*, \mathcal{T}^*, \mathcal{M}^*, \mathcal{K}^*) = \left(\frac{s}{\mu - p\frac{\mathcal{T}^*}{h+\mathcal{T}^*} + m\mathcal{T}^* + K_{\mathcal{E}}\frac{V_m}{\gamma}}, \mathcal{T}^*, \frac{V_m}{\gamma}, \frac{\lambda}{\delta}\mathcal{T}^*\right),$$

   where $\mathcal{T}^*$ satisfies $\xi(\mathcal{T}^* + g)\left[\mu - p\frac{\mathcal{T}^*}{h+\mathcal{T}^*} + m\mathcal{T}^* + K_{\mathcal{E}}\frac{V_m}{\gamma}\right] - as = 0$, i.e., after multiplication by $(h + \mathcal{T}^*)$,

   $$A\mathcal{T}^{*3} + B\mathcal{T}^{*2} + C\mathcal{T}^* + D = 0. \tag{5.1}$$

With
$A = m\xi$,
$B = \xi\left[K_{\mathcal{E}}\frac{V_m}{\gamma} + m(g+h) + \mu - p\right]$,
$C = \xi\left[K_{\mathcal{E}}\frac{V_m}{\gamma}(g+h) + gh\,m + g(\mu - p) + h\mu\right] - as$,
$D = h\left[\xi g\left(\mu + K_{\mathcal{E}}\frac{V_m}{\gamma}\right) - as\right]$,
$\xi = r\left(1 - \frac{\delta}{\lambda}\right) - K_{\mathcal{T}}\frac{V_m}{\gamma}$.

Remark 7. *This is the endemic equilibrium point, corresponding to the coexistence of a persistent tumor and a nonzero immune response. In this situation, the carrying capacity is slaved to the tumor through $\mathcal{K}^* = \frac{\lambda}{\delta}\mathcal{T}^*$. We show in Proposition 3 that such an equilibrium exists only when $\xi > 0$, hence only when $\lambda > \delta$; under hypotheses $(H1)$ and $(H2)$ used to establish boundedness, it does not exist, and the system possesses only the tumor-free equilibria E_0 and E_1.*

Remark 8 (The field at the tumor-free equilibria)**.** *The points E_0 and E_1 both have $\mathcal{K} = 0$, where the term $r\mathcal{T}^2/\mathcal{K}$ of the second equation and the Jacobian entry $r\mathcal{T}^2/\mathcal{K}^2$ are of the indeterminate form $0/0$; strictly speaking, these points do not belong to the open set on which $\mathcal{F}$ is defined. We resolve this singularity rigorously via the blow-up $v = \mathcal{T}/\mathcal{K}$(well-defined for $\mathcal{K} > 0$), which transforms the singular system into the smooth system*

$$\dot{v} = v\left[r + \delta - K_{\mathcal{T}}\mathcal{M} - \frac{a\mathcal{E}}{g + v\mathcal{K}} - (r+\lambda)v\right],$$

a smooth ODE at $v = \mathcal{K} = 0$. Linearising at $v = 0$ shows that the eigenvalue associated with the $\mathcal{T}/\mathcal{K}$-direction is $\mu_v = r + \delta - K_{\mathcal{T}}\mathcal{M}^* - a\mathcal{E}^*/g = \rho + \delta$, where ρ denotes the eigenvalue obtained by naively setting $r\mathcal{T}^2/\mathcal{K} = r\mathcal{T}^2/\mathcal{K}^2 = 0$. Stability along this direction therefore requires the strictly stronger condition $\rho < -\delta$, not merely $\rho < 0$. All statements concerning E_0 and E_1 below use this corrected condition.

The Jacobian matrix of system (2.1) is given by

$$J = \begin{pmatrix} -\mu + p\frac{\mathcal{T}}{h+\mathcal{T}} - m\mathcal{T} - K_{\mathcal{E}}\mathcal{M} & p\frac{\mathcal{E}h}{(h+\mathcal{T})^2} - m\mathcal{E} & -K_{\mathcal{E}}\mathcal{E} & 0 \\ -a\frac{\mathcal{T}}{g+\mathcal{T}} & r(1-\frac{2\mathcal{T}}{\mathcal{K}}) - \frac{a\mathcal{E}g}{(g+\mathcal{T})^2} - K_{\mathcal{T}}\mathcal{M} & -K_{\mathcal{T}}\mathcal{T} & \frac{r\mathcal{T}^2}{\mathcal{K}^2} \\ 0 & 0 & -\gamma & 0 \\ 0 & \lambda & 0 & -\delta \end{pmatrix}. \tag{5.2}$$

Proposition 1. *The equilibrium point E_0 always exists and is locally asymptotically stable if $V_m > \frac{(r+\delta)\gamma}{K_{\mathcal{T}}}$, i.e., a sufficiently high rate of externally administered treatment is required. However, this may lead to adverse side effects, making such a scenario biologically rare.*

Proof. The Jacobian matrix of (2.1) in E_0 is

$$J(E_0) = \begin{pmatrix} -\mu - K_{\mathcal{E}}\frac{V_m}{\gamma} & 0 & 0 & 0 \\ 0 & r - K_{\mathcal{T}}\frac{V_m}{\gamma} & 0 & 0 \\ 0 & 0 & -\gamma & 0 \\ 0 & \lambda & 0 & -\delta \end{pmatrix}.$$

The eigenvalues associated with the regular directions are

$$\lambda_1 = -\gamma, \quad \lambda_2 = -\delta, \quad \lambda_3 = -(\mu + K_{\mathcal{E}}\frac{V_m}{\gamma}),$$

and, along the $\mathcal{T}/\mathcal{K}$-direction (Remark above), $\mu_v = r+\delta-K_{\mathcal{T}}\frac{V_m}{\gamma}$. E_0 is locally asymptotically stable if and only if all eigenvalues are strictly negative. The first three eigenvalues are always strictly negative; the condition therefore reduces to $\mu_v < 0$, that is, $V_m > \dfrac{(r+\delta)\gamma}{K_{\mathcal{T}}}$. We emphasize that the inequality must be *strict*: The borderline case $\mu_v = 0$ yields a non-hyperbolic equilibrium for which linearization is inconclusive. □

Proposition 2. *The equilibrium point E_1 exists and is locally asymptotically stable if and only if*

$$r+\delta < \frac{a}{g}\left(\frac{s}{\mu + K_{\mathcal{E}}\frac{V_m}{\gamma}}\right) + K_{\mathcal{T}}\frac{V_m}{\gamma}.$$

This condition implies that tumor control is achieved only if the combined effects of treatment and the immune response are stronger than tumor growth. Consequently, even if residual tumor cells are present, they cannot proliferate due to the combined strength of the therapeutic intervention together with the immune system.

Proof. The Jacobian matrix of (2.1) in E_1 is

$$J(E_1) = \begin{pmatrix} -\left(\mu + K_{\mathcal{E}}\frac{V_m}{\gamma}\right) & \frac{(p-mh)s}{(\mu+K_{\mathcal{E}}\frac{V_m}{\gamma})h} & -\frac{K_{\mathcal{E}}s}{\mu+K_{\mathcal{E}}\frac{V_m}{\gamma}} & 0 \\ 0 & r - \frac{a}{g}\left(\frac{s}{\mu+K_{\mathcal{E}}\frac{V_m}{\gamma}}\right) - K_{\mathcal{T}}\frac{V_m}{\gamma} & 0 & 0 \\ 0 & 0 & -\gamma & 0 \\ 0 & \lambda & 0 & -\delta \end{pmatrix}$$

The eigenvalues associated with the regular directions are

$$\lambda_1 = -\left(\mu + K_{\mathcal{E}}\frac{V_m}{\gamma}\right), \quad \lambda_2 = -\gamma, \quad \lambda_4 = -\delta,$$

and, along the $\mathcal{T}/\mathcal{K}$-direction (Remark above),

$$\mu_v = r + \delta - \frac{a}{g}\left(\frac{s}{\mu + K_{\mathcal{E}}\frac{V_m}{\gamma}}\right) - K_{\mathcal{T}}\frac{V_m}{\gamma}.$$

The diagonal entry of the first row of $J(E_1)$ is $-\mu + p\frac{\mathcal{T}}{h+\mathcal{T}} - m\mathcal{T} - K_{\mathcal{E}}\mathcal{M}$ evaluated at $\mathcal{T} = 0$ and $\mathcal{M} = V_m/\gamma$, that is $-(\mu + K_{\mathcal{E}}V_m/\gamma)$ and not $-\mu$; the eigenvalue λ_1 has been corrected accordingly. The eigenvalues λ_1, $\lambda_2 = -\gamma$ and $\lambda_4 = -\delta$ are always strictly negative, since $\mu, \gamma, \delta, K_{\mathcal{E}}, V_m > 0$. The only eigenvalue μ_v is negative if and only if

$$r+\delta < \frac{a}{g}\left(\frac{s}{\mu + K_{\mathcal{E}}\frac{V_m}{\gamma}}\right) + K_{\mathcal{T}}\frac{V_m}{\gamma}.$$

Therefore, E_1 is locally asymptotically stable if and only if the above condition holds. □

Proposition 3. *Let* $\xi := r\left(1 - \frac{\delta}{\lambda}\right) - K_{\mathcal{T}}\frac{V_m}{\gamma}$.

(1) *If* $A \cdot D < 0$*, the cubic* (5.1) *possesses at least one root* $\mathcal{T}^* > 0$*; the corresponding point* $(\mathcal{E}^*, \mathcal{T}^*, \mathcal{M}^*, \mathcal{K}^*)$ *has all its coordinates strictly positive, and is therefore a biologically admissible endemic equilibrium, if and only if* $\xi > 0$.

(2) *Under hypotheses* $(H1)$ *and* $(H2)$ *of Lemma 2, no endemic equilibrium exists: The only equilibria of* (2.1) *are the tumor-free points* E_0 *and* E_1.

Proof. Using Eq (5.1), the equilibrium exists if $A \cdot D < 0$, and we distinguish two cases

- $A < 0$ **and** $D > 0$: this means $\xi < 0$, together with $\xi g\left(\mu + K_{\mathcal{E}}\frac{V_m}{\gamma}\right) - as > 0$.
- $A > 0$ **and** $D < 0$: this means $\xi > 0$ together with $\xi g\left(\mu + K_{\mathcal{E}}\frac{V_m}{\gamma}\right) - as < 0$.

In both cases $P(\mathcal{T}) = A\mathcal{T}^3 + B\mathcal{T}^2 + C\mathcal{T} + D$ is continuous on $[0, +\infty)$ with $P(0) = D$ and $P(\mathcal{T}) \to \text{sign}(A) \cdot (+\infty)$ as $\mathcal{T} \to +\infty$, so the two limits have opposite signs and the intermediate value theorem guarantees the existence of a root $\mathcal{T}^* \in (0, +\infty)$. We stress that $A \cdot D < 0$ is sufficient but not necessary: A positive root may also exist when $A \cdot D > 0$; for instance, when P has two positive roots.

Biological admissibility further requires $\mathcal{E}^* > 0$. Since $\mathcal{T}^* = -g + a\mathcal{E}^*/\xi$, one has $\mathcal{E}^* = \xi(\mathcal{T}^* + g)/a$ with $a, g, \mathcal{T}^* > 0$, so $\mathcal{E}^* > 0$ if and only if $\xi > 0$; this proves part (1). No additional condition on μ is needed: With the expression of $\mathcal{E}^*$ given above, the denominator $\mu - p\frac{\mathcal{T}^*}{h+\mathcal{T}^*} + m\mathcal{T}^* + K_{\mathcal{E}}\frac{V_m}{\gamma}$ exceeds $\mu - p > 0$ under $(H1)$, because

$$p\frac{\mathcal{T}^*}{h + \mathcal{T}^*} < p.$$

Proof of part (2). Under $(H2)$ we have $\lambda < \delta$, hence $\delta/\lambda > 1$ and

$$\xi = r\left(1 - \frac{\delta}{\lambda}\right) - K_{\mathcal{T}}\frac{V_m}{\gamma} < 0.$$

Under $(H1)$, $\mu - p > 0$, and each of the four quantities

$$m, \qquad K_{\mathcal{E}}\frac{V_m}{\gamma} + m(g + h) + \mu - p, \qquad K_{\mathcal{E}}\frac{V_m}{\gamma}(g + h) + ghm + g(\mu - p) + h\mu, \qquad g\left(\mu + K_{\mathcal{E}}\frac{V_m}{\gamma}\right)$$

is strictly positive. Since A and B are equal to ξ times positive quantities, and $C = \xi Q - as$, where $Q > 0$ and $as > 0$, while

$$D = h\left[\xi g\left(\mu + \frac{K_E V_m}{\gamma}\right) - as\right]$$

with $\xi < 0$, all four coefficients are strictly negative. Hence,

$$P(T) < 0 \qquad \text{for every } T > 0.$$

The cubic has no positive root and no endemic equilibrium exists. In particular $A \cdot D > 0$, so part (1) does not apply.

Tumor persistence at a steady state and boundedness of the solutions are therefore mutually exclusive in this model: In the regime in which Lemma 2 guarantees bounded trajectories, only the tumor-free equilibria survive. This is confirmed numerically in the next subsection. □

Proposition 4. *The endemic equilibrium E^* is locally asymptotically stable if and only if*

$$a_1 > 0, \qquad a_3 > 0, \qquad a_1 a_2 > a_3.$$

with

$$a_1 = \delta - J_{11} - J_{22}$$

$$a_2 = J_{11}J_{22} - J_{12}J_{21} - \delta(J_{11} + J_{22}) - \lambda J_{24}$$

$$a_3 = \delta(J_{11}J_{22} - J_{12}J_{21}) + \lambda J_{11}J_{24}$$

where

$$J_{11} = -\mu + p\frac{\mathcal{T}^*}{h + \mathcal{T}^*} - m\mathcal{T}^* - K_{\mathcal{E}}\mathcal{M}^*, \qquad J_{12} = p\frac{\mathcal{E}^* h}{(h + \mathcal{T}^*)^2} - m\mathcal{E}^*, \qquad J_{13} = -K_{\mathcal{E}}\mathcal{E}^*,$$

$$J_{21} = -a\frac{\mathcal{T}^*}{g + \mathcal{T}^*}, \qquad J_{22} = r\left(1 - \frac{2\mathcal{T}^*}{\mathcal{K}^*}\right) - \frac{a\mathcal{E}^* g}{(g + \mathcal{T}^*)^2} - K_{\mathcal{T}}\mathcal{M}^*, \qquad J_{24} = \frac{r\mathcal{T}^{*2}}{\mathcal{K}^{*2}}.$$

Proof. The third row of the Jacobian is $(0, 0, -\gamma, 0)$, so the treatment variable decouples in the linearization and $\Lambda = -\gamma < 0$ is always an eigenvalue. Deleting the third row and the third column leaves

$$\widetilde{J} = \begin{pmatrix} J_{11} & J_{12} & 0 \\ J_{21} & J_{22} & J_{24} \\ 0 & \lambda & -\delta \end{pmatrix},$$

and expanding $\det(\widetilde{J} - \Lambda I)$ along the first column gives

$$\det(\widetilde{J} - \Lambda I) = (J_{11} - \Lambda)\big[(J_{22} - \Lambda)(-\delta - \Lambda) - \lambda J_{24}\big] + J_{12}J_{21}(\delta + \Lambda).$$

Expanding and changing sign yields $\Lambda^3 + a_1\Lambda^2 + a_2\Lambda + a_3 = 0$ with the coefficients given above. Since J_{13} and J_{23} belong to the deleted column, they cannot appear in any a_i. By the Routh–Hurwitz criterion for a cubic with real coefficients, all its roots have strictly negative real part if and only if $a_1 > 0$, $a_3 > 0$ and $a_1 a_2 > a_3$. Together with $-\gamma < 0$, these conditions give local asymptotic stability under exactly these three conditions. The coefficients were obtained and then verified by symbolic computation. □

Remark 9. *These inequalities give explicit, checkable conditions in terms of the model parameters. In particular,* $a_1 > 0$ *requires the trace condition* $J_{11} + J_{22} < \delta$*: The combined self-regulation of the effector and tumor compartments must dominate the decay rate of the carrying capacity. The term* $-\lambda J_{24}$ *appearing in* a_2 *shows explicitly how the tumor-driven vascularization* λ *acts against stability, which is the mathematical counterpart of the sensitivity result* $\mathrm{PRCC}(\lambda) > 0$ *obtained in Section 7.*

Numerical illustration. We take the parameter set $s = 10000$, $\mu = 0.04$, $p = 0.015$, $h = 20$, $m = 2 \times 10^{-11}$, $K_{\mathcal{E}} = 0.09$, $r = 0.0005$, $a = 3.41 \times 10^{-10}$, $g = 1000$, $K_{\mathcal{T}} = 0.9$, $\gamma = 0.2$, $\lambda = 0.1$, and $\delta = 0.5$, with the initial values $\mathcal{E}(0) = 500$, $\mathcal{T}(0) = 10^4$, $\mathcal{M}(0) = \frac{V_m}{\gamma}$, and $\mathcal{K}(0) = \frac{\lambda}{\delta}\mathcal{T}_0$.

Numerical study of the local stability. With the parameter set above, one has $K_{\mathcal{T}} V_m/\gamma = 0.9 \times 2.5 = 2.25$ for $V_m = 0.5$, whereas $r = 5 \times 10^{-4}$: The drug–induced tumor–cell kill rate exceeds the proliferation rate by more than three orders of magnitude, so $\xi < 0$ and, by Proposition 3(2), no endemic equilibrium exists. The relevant attractor is the tumor-free equilibrium E_1.

The equilibria have been recomputed exactly (see Table 1):

Table 1. Tumor-free equilibrium E_1 and its eigenvalues, recomputed.

	$V_m = 0.5$	$V_m = 10$
$E_1 = (\mathcal{E}_1, 0, V_m/\gamma, 0)$	(37735.85, 0, 2.5, 0)	(2202.64, 0, 50, 0)
eigenvalues	$-0.2650,\ -1.7495,\ -0.2,\ -0.5$	$-4.5400,\ -44.4995,\ -0.2,\ -0.5$

In both cases, all four eigenvalues are strictly negative, so E_1 is locally asymptotically stable, in agreement with Proposition 2. Note that $\lambda_1 = -(\mu + K_{\mathcal{E}} V_m/\gamma)$ equals -0.265 and -4.54, respectively, and not $-\mu = -0.04$; this is the correction recorded above.

High-intensity treatment scenario: Increasing the dose to $V_m = 10$ does not affect the existence of solutions, Theorem 1 holds for every admissible V_m, but it moves the system further into the regime $\xi < 0$, in which Proposition 3(2) forbids any endemic equilibrium. The relevant equilibrium remains E_1, whose coordinates and eigenvalues are given in Table 1; the convergence is faster because $|\lambda_2|$ increases from 1.7495 to 44.4995.

Figures 1 and 2 illustrate the evolution of different system components around the equilibrium point. In both figures, the system converges to the equilibrium, confirming its local stability. However, convergence is faster in Figure 2, where a higher treatment level is administered.

Remark 10.

1) *The stability and existence of this equilibrium depend on the parameters listed below.*

2) *Stability is achieved when the treatment rate Vm is sufficiently large while remaining within biologically and clinically admissible bounds.*

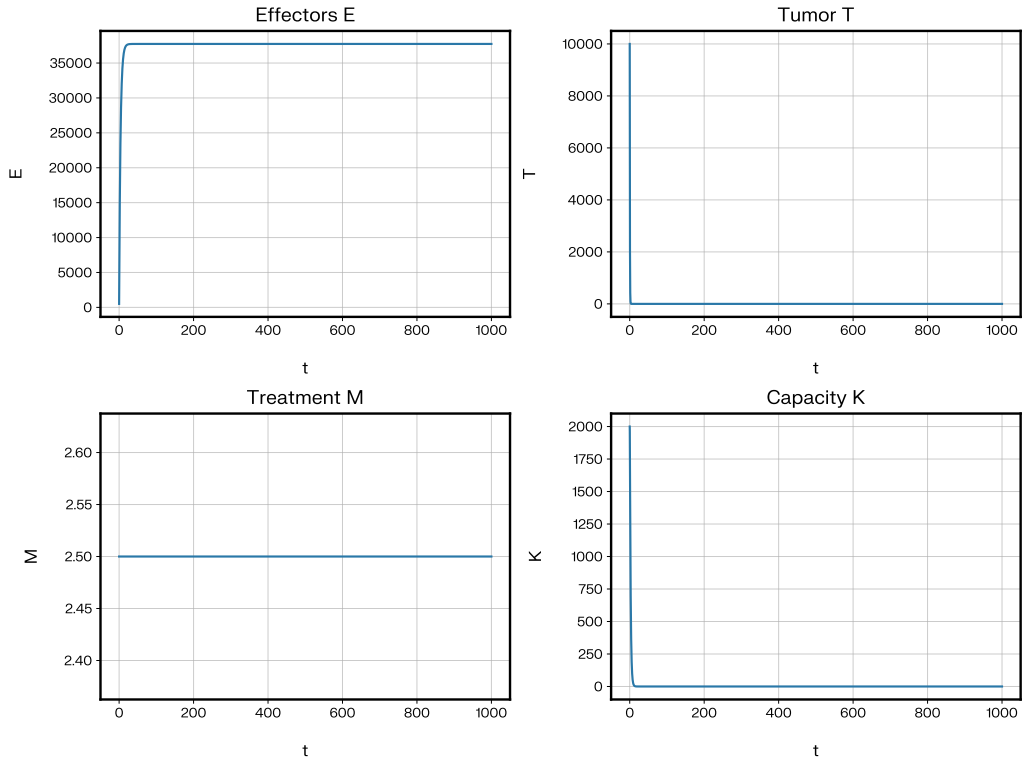

Figure 1. States evolution around equilibrium point, $V_m = 0.5$.

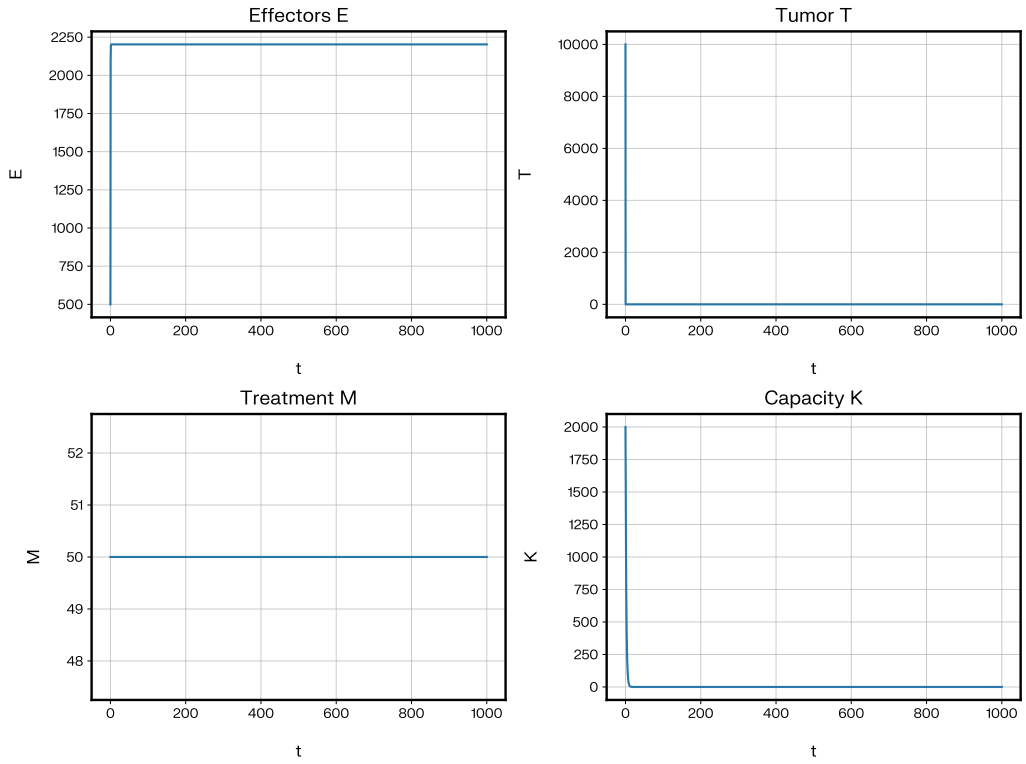

Figure 2. States evolution around equilibrium point, $V_m = 10$.

6. Optimal control analysis

Control theory studies the behavior of dynamical systems under the influence of external inputs, aiming to drive the system from an initial state to a desired final state using appropriate control signals. This branch of mathematics is applied to multiple disciplines, including medical sciences, and specifically oncology. Dynamical tumor models aim to better understand the interactions among tumor cells, the immune system, and treatment. Inspired by epidemiological models, such approaches consider different cell populations that are modeled using differential equations.

Our objective of this work is to minimize the tumor–cell population, maximize the effector–cell population, and maintain an optimal treatment dose.

The objective function is given by

$$\mathcal{J}(V_m) = \int_0^{T_f} \left(\alpha_{\mathcal{T}} \mathcal{T}(t) - \alpha_{\mathcal{E}} \mathcal{E}(t) + \frac{\alpha_u}{2} V_m(t)^2 \right) dt + \omega_{\mathcal{T}} \mathcal{T}(T_f),$$

where

- The control $V_m(t)$, $t \in [0, T_f]$, is the rate at which drug is administered from outside the body. Following the referees' suggestion, we use the symbol V_m throughout, consistently with the parameter list of Section 2, instead of the generic notation u.
- T_f is the fixed final time.
- $\alpha_{\mathcal{E}}$, $\alpha_{\mathcal{T}}$ and α_u are positive weights.
- $\omega_{\mathcal{T}} \mathcal{T}(T_f)$ is the residual tumor burden at a final time T_f.
- In the numerical experiments, we take $T_f = 100$, $V_m^{\max} = 1$, $\alpha_{\mathcal{T}} = 1$, $\alpha_{\mathcal{E}} = 0.5$, $\alpha_u = 5 \times 10^5$, and $\omega_{\mathcal{T}} = 0.9$, with initial data $E_0 = 500$, $T_0 = 10^4$, $M_0 = 0$, and $K_0 = (\lambda/\delta)\, T_0$.

Remark 11.

- *$\alpha_{\mathcal{T}} \mathcal{T}$ weights the tumor size (minimize the number of tumor cells).*
- *$\alpha_{\mathcal{E}} \mathcal{E}$ assigns value to the presence of immuno–effector cells (maximize the number of immuno–effector cells).*
- *$\frac{\alpha_u}{2} V_m(t)^2$ limits the dose of the treatment to avoid problems such as toxicity and side effects.*
- *The choice of dividing the previous term by 2 is conventional; it simplifies the differentiation of the Hamiltonian.*

The optimal control problem considered is:

$$\begin{cases} \mathcal{J}(V_m) = \displaystyle\int_0^{T_f} \left(\alpha_{\mathcal{T}}\mathcal{T}(t) - \alpha_{\mathcal{E}}\mathcal{E}(t) + \frac{\alpha_u}{2}V_m(t)^2\right)dt + \omega_{\mathcal{T}}\mathcal{T}(T_f) \to \min_{V_m}, \\ \frac{d\mathcal{E}}{dt} = s - \mu\mathcal{E} + p\frac{\mathcal{E}\mathcal{T}}{h+\mathcal{T}} - m\mathcal{E}\mathcal{T} - K_{\mathcal{E}}\mathcal{M}\mathcal{E}, \\ \frac{d\mathcal{T}}{dt} = r\mathcal{T}\left(1 - \frac{\mathcal{T}}{\mathcal{K}}\right) - a\frac{\mathcal{E}\mathcal{T}}{g+\mathcal{T}} - K_{\mathcal{T}}\mathcal{M}\mathcal{T}, \\ \frac{d\mathcal{M}}{dt} = -\gamma\mathcal{M} + V_m(t), \\ \frac{d\mathcal{K}}{dt} = \lambda\mathcal{T} - \delta\mathcal{K}, \\ 0 \le V_m(t) \le V_m^{\max}, \qquad t \in [0, T_f]. \end{cases} \tag{6.1}$$

where T_f is a fixed final time chosen for the simulations.

Set of admissible controls. Let $V_m^{\max} > 0$ be a fixed upper bound prescribed by the maximum tolerated dose. We define

$$\mathcal{U}_{ad} := \left\{V_m \in L^\infty(0, T_f) \ : \ 0 \le V_m(t) \le V_m^{\max} \text{ for a.e. } t \in [0, T_f]\right\}.$$

$\mathcal{U}_{ad}$ is non-empty (it contains $V_m \equiv 0$), convex, closed and bounded in $L^\infty(0, T_f)$, and is therefore weakly-$*$ compact.

Theorem 2. *There exists an optimal control $V_m^* \in \mathcal{U}_{ad}$ and a corresponding optimal trajectory, solution of* (6.1)*, at which $\mathcal{J}$ attains its minimum over $\mathcal{U}_{ad}$.*

Proof. We verify the hypotheses of the Filippov–Cesari existence theorem one by one.

(i) *The admissible set is non-empty and the states are well defined.* $V_m \equiv 0$ belongs to $\mathcal{U}_{ad}$, and by Theorem 1, every $V_m \in \mathcal{U}_{ad}$ produces a unique solution of (2.1) on $[0, T_f]$.

(ii) *$\mathcal{U}_{ad}$ is convex and weakly-$*$ compact*, as observed above.

(iii) *Uniform boundedness of the trajectories.* By Lemma 2, all states remain in the compact set Ω, with bounds depending only on the data and on $V_m^{\max}$; hence, these bounds are uniform for all $V_m \in \mathcal{U}_{ad}$.

(iv) *Convexity and compactness of the velocity set.* The control enters the dynamics affinely, only through the term $+V_m$ in the third equation, so for each state, X the set $\{\mathcal{F}(X, V_m) : V_m \in [0, V_m^{\max}]\}$ is a compact segment, meaning convex.

(v) *Convexity of the integrand in the control.* The running cost $\alpha_{\mathcal{T}}\mathcal{T} - \alpha_{\mathcal{E}}\mathcal{E} + \frac{\alpha_u}{2}V_m^2$ is strictly convex in V_m since $\alpha_u > 0$.

Taking a minimizing sequence $(V_m^k) \subset \mathcal{U}_{ad}$, weak-$*$ compactness gives a subsequence converging weakly-$*$ to some $V_m^* \in \mathcal{U}_{ad}$; by (iii) and the Arzelà–Ascoli theorem the associated states converge uniformly to the state associated with V_m^*, and weak lower semicontinuity of convex integral functionals gives $\mathcal{J}(V_m^*) \leq \liminf_k \mathcal{J}(V_m^k)$. Hence, the infimum is attained. □

The Hamiltonian of the system (6.1), is given for $t \in [0, T_f]$ by:

$$\mathcal{H} = p_{\mathcal{E}}(s - \mu\mathcal{E} + p\frac{\mathcal{E}\mathcal{T}}{h+\mathcal{T}} - m\mathcal{E}\mathcal{T} - K_{\mathcal{E}}\mathcal{M}\mathcal{E}) + p_{\mathcal{T}}(r\mathcal{T}(1 - \frac{\mathcal{T}}{\mathcal{K}}) - a\frac{\mathcal{E}\mathcal{T}}{g+\mathcal{T}} - K_{\mathcal{T}}\mathcal{M}\mathcal{T})$$

$$+p_{\mathcal{M}}(-\gamma\mathcal{M} + V_m) + p_{\mathcal{K}}(\lambda\mathcal{T} - \delta\mathcal{K}) + \alpha_{\mathcal{T}}\mathcal{T} - \alpha_{\mathcal{E}}\mathcal{E} + \frac{\alpha_u}{2}{V_m}^2.$$

The adjoint variables are defined as follows: $p_{\mathcal{E}}, p_{\mathcal{T}}, p_{\mathcal{M}}$, and $p_{\mathcal{K}}$ satisfy for each $t \in [0, T_f]$

$$\begin{cases} \dot{p_{\mathcal{E}}} = (\mu - \frac{p\mathcal{T}}{h+\mathcal{T}} + m\mathcal{T} + K_{\mathcal{E}}\mathcal{M})p_{\mathcal{E}} + (\frac{a\mathcal{T}}{g+\mathcal{T}})p_{\mathcal{T}} + \alpha_{\mathcal{E}}, \\ \dot{p_{\mathcal{T}}} = \left(m\mathcal{E} - \frac{ph\mathcal{E}}{(h+\mathcal{T})^2}\right)p_{\mathcal{E}} + \left(-r + \frac{2r\mathcal{T}}{\mathcal{K}} + \frac{a\mathcal{E}g}{(g+\mathcal{T})^2} + K_{\mathcal{T}}\mathcal{M}\right)p_{\mathcal{T}} - \lambda p_{\mathcal{K}} - \alpha_{\mathcal{T}}, \\ \dot{p_{\mathcal{M}}} = K_{\mathcal{E}}\mathcal{E}p_{\mathcal{E}} + K_{\mathcal{T}}\mathcal{T}p_{\mathcal{T}} + \gamma p_{\mathcal{M}}, \\ \dot{p_{\mathcal{K}}} = -\frac{r\mathcal{T}^2}{\mathcal{K}^2}p_{\mathcal{T}} + \delta p_{\mathcal{K}}. \end{cases}$$

The transversality conditions are:

$$p_{\mathcal{E}}(T_f) = p_{\mathcal{M}}(T_f) = p_{\mathcal{K}}(T_f) = 0, \qquad p_{\mathcal{T}}(T_f) = \omega_{\mathcal{T}}.$$

By minimizing the Hamiltonian with respect to the control and using the boundary and transversality conditions, we obtain the following projection formula for the optimal control:

$$V_m^* = \min\left\{\max\left\{0, -\frac{p_{\mathcal{M}}}{\alpha_u}\right\}, V_m^{\max}\right\}.$$

Since $\mathcal{J}$ is minimized and $\mathcal{H}$ is strictly convex in the control, the Pontryagin condition is a pointwise minimization and not a maximization; the previous wording has been corrected.

Remark 12 (Structure of the optimal control)**.** *The running cost contains the strictly convex term $\frac{\alpha_u}{2}V_m^2$ with $\alpha_u > 0$, so the Hamiltonian is strictly convex in the control and its pointwise minimiser is single-valued. Since $p_{\mathcal{M}}$ is absolutely continuous, the projection formula above shows that V_m^* is a* continuous*, piecewise smooth function of t: It consists of interior arcs on which $V_m^* = -p_{\mathcal{M}}/\alpha_u$, separated by saturated arcs on which $V_m^* = 0$ or $V_m^* = V_m^{\max}$. A genuine bang–bang structure can occur only when the Hamiltonian is affine in the control, that is when $\alpha_u = 0$, which is not the case here. The previous version described the control as bang–bang while displaying the formula above, which exhibits a continuous dependence on $p_{\mathcal{M}}$; the term has been removed throughout and the discussions of Figures 4 and 6 rewritten accordingly.*

Numerical methods

(a) Direct method (discretize-then-optimize). The interval $[0, T_f]$ is divided into $N = 1000$ equal subintervals of length $\Delta t = T_f/N$. The state equations are discretized by an explicit fourth-order Runge–Kutta scheme and the control is approximated by a piecewise-constant function on each subinterval. The integral cost is evaluated by the composite Simpson rule. This reduces (6.1) to a finite-dimensional nonlinear program in $(V_{m,0}, \ldots, V_{m,N-1}) \in [0, V_m^{\max}]^N$, solved in MATLAB with `fmincon`, using a sequential quadratic programming algorithm, with gradients supplied by finite differences, optimality and feasibility tolerances set to 10^{-8}, and initial guess $V_m \equiv V_m^{\max}/2$.

(b) Indirect method (single shooting). The optimality system consists of the four state equations with their initial conditions, the four adjoint equations with the transversality conditions $p_{\mathcal{E}}(T_f) = p_{\mathcal{M}}(T_f) = p_{\mathcal{K}}(T_f) = 0$, $p_{\mathcal{T}}(T_f) = \omega_{\mathcal{T}}$, and the projection formula for the control. The unknown initial adjoint vector $p(0)$ is taken as the shooting variable; the full eight-dimensional system is integrated forward with `ode45` (relative tolerance 10^{-10}, absolute tolerance 10^{-12}), and the residual of the four terminal conditions is driven to zero with `fsolve`. The initial guess for $p(0)$ is taken from the adjoint values returned by the direct method, which we found essential for convergence; convergence is declared when the terminal residual norm falls below 10^{-10}.

(c) Cross-validation. The two methods are independent: The direct method is robust but has limited accuracy, whereas shooting is highly accurate once a good initial guess is available. The relative difference between the two computed optimal costs is below 10^{-6}, which supports the correctness of both implementations. This is why both are reported.

The following figures show the evolution of the system states using a direct method first and then an indirect method.

Figure 3 illustrates the temporal evolution of the different compartments in our optimal control problem (6.1). We observe a rapid decrease in both tumor cells and their carrying capacity, accompanied by an increase in effector immune cells. Once the tumor has been essentially eradicated, the effector population continues to rise while the administered drug concentration decays, since the control is no longer active. The control (treatment) is continuous and bounded: It starts from an interior value strictly below the admissible bound $V_m^{\max}$ and then decreases continuously toward zero, after which it remains equal to zero once the immune response is sufficiently strong and the tumor is essentially eradicated, making further treatment unnecessary and costly.

Figure 4 presents the temporal evolution of the control, representing the administered treatment. The optimal control starts from an interior value strictly below the admissible bound $V_m^{\max}$ and decreases continuously toward zero over a short initial window, after which it remains equal to zero; the upper bound $V_m^{\max}$ is not active at the optimum for this parameter set. Since the running cost contains the strictly convex term $\frac{\alpha_u}{2} V_m^2$ with $\alpha_u > 0$, the pointwise minimizer of the Hamiltonian is single-valued and equals the continuous function $V_m^* = \min\{\max\{0, -p_{\mathcal{M}}/\alpha_u\}, V_m^{\max}\}$; since $p_{\mathcal{M}}$ is absolutely continuous, the control is a genuinely continuous function of time and not a bang–bang one. The decrease occurs over a short time window, so that at the scale of the full horizon it appears steep; this sharpness reflects the brevity of the continuous transition and not a true discontinuity. Thus, the numerical solution indicates an initial treatment phase, a brief continuous decrease, and treatment cessation. This figure is consistent with the description of the trajectories presented in Figure 3.

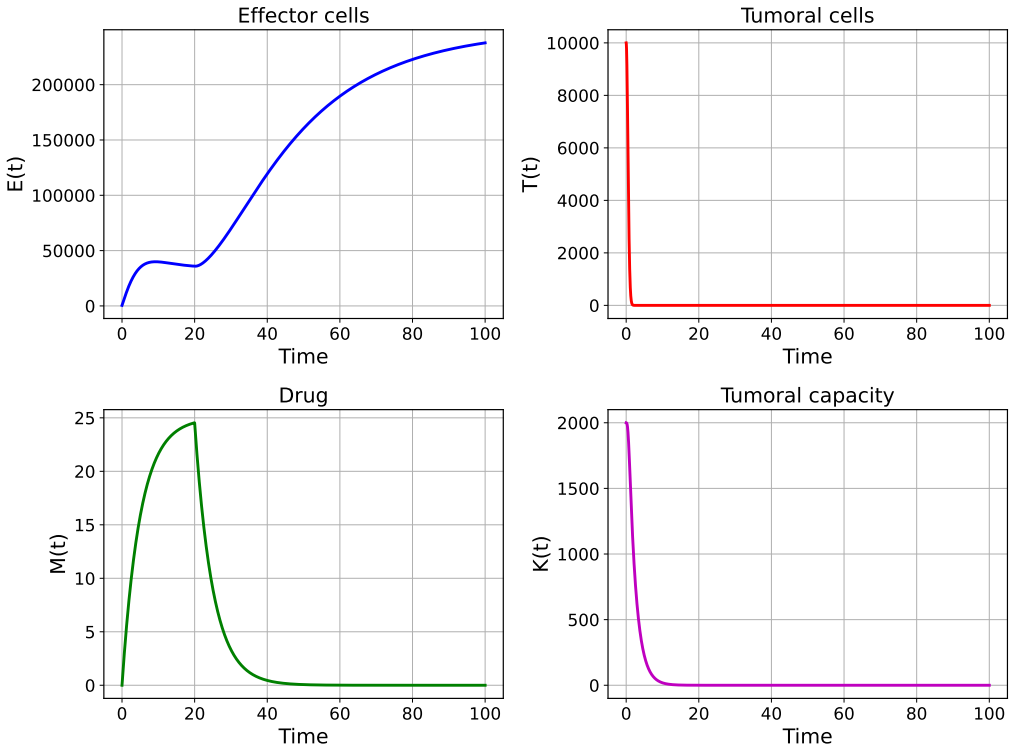

Figure 3. State evolution of the solutions using a direct method.

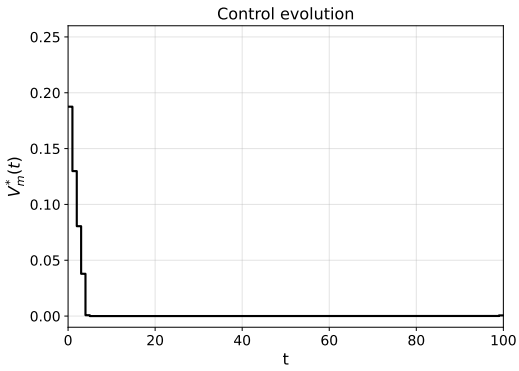

Figure 4. Control evolution using a direct method.

We observe that the results shown in Figures 5 and 6 are very similar to those presented above. The indirect method provides higher precision, whereas the direct method, given the moderate complexity of our system, is faster and computationally more efficient. Both numerical approaches lead to qualitatively consistent optimal treatment profiles and to optimal cost values that agree to within a relative difference below 10^{-6}. The upper bound $V_m^{\max}$ is not active at the optimum for this parameter set: The direct (piecewise-constant) approximation attains a maximum of about 0.19, while the continuous reconstruction from the indirect method attains about 0.22. This small difference reflects the distinct numerical representations of the control (a piecewise-constant approximation on the optimisation grid versus a continuous adjoint-based reconstruction on the dense integration grid), and

does not affect the continuous structure of the optimal control nor the value of the objective functional.

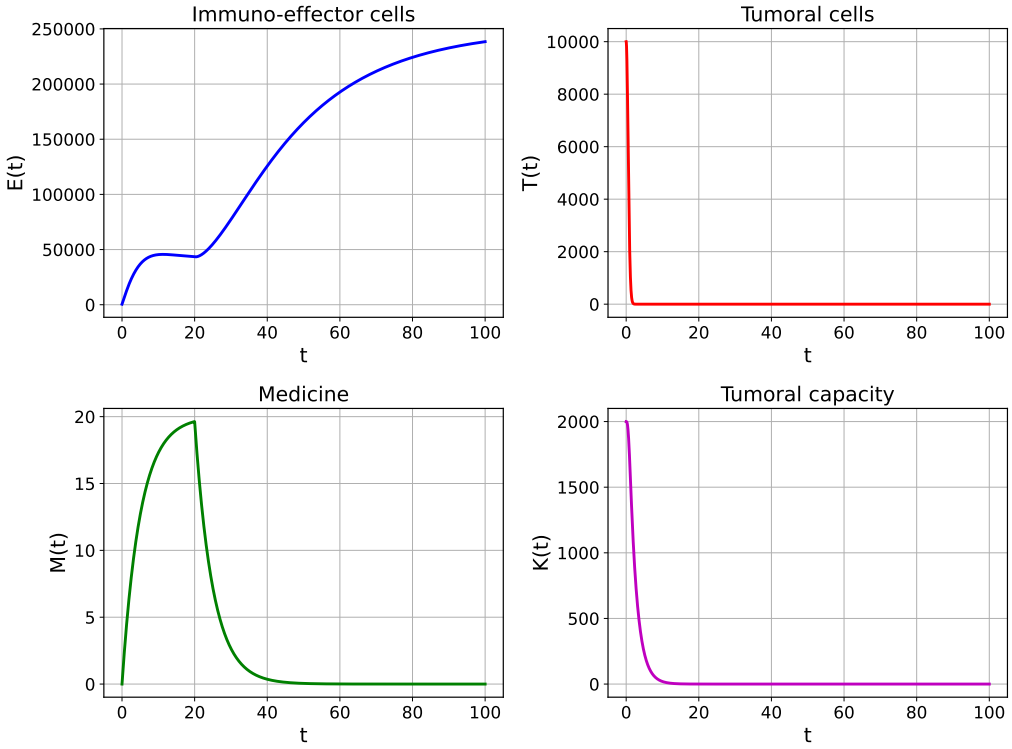

Figure 5. State evolution of the solutions using an indirect method.

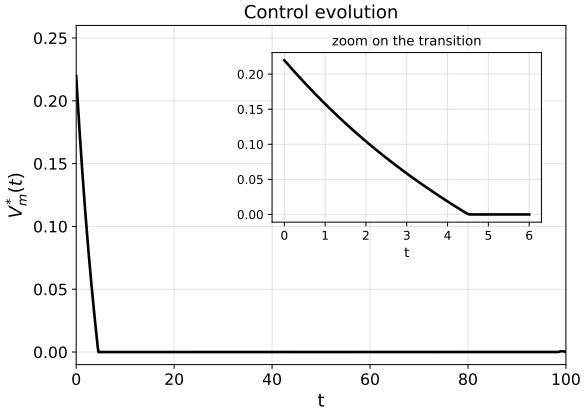

Figure 6. Control evolution using an indirect method.

6.1. Treatment comparison

In the following section, we consider different treatment types and dosages for the same cancer type. The problem setup and parameters are the same as previously described. The results are presented in the following figures.

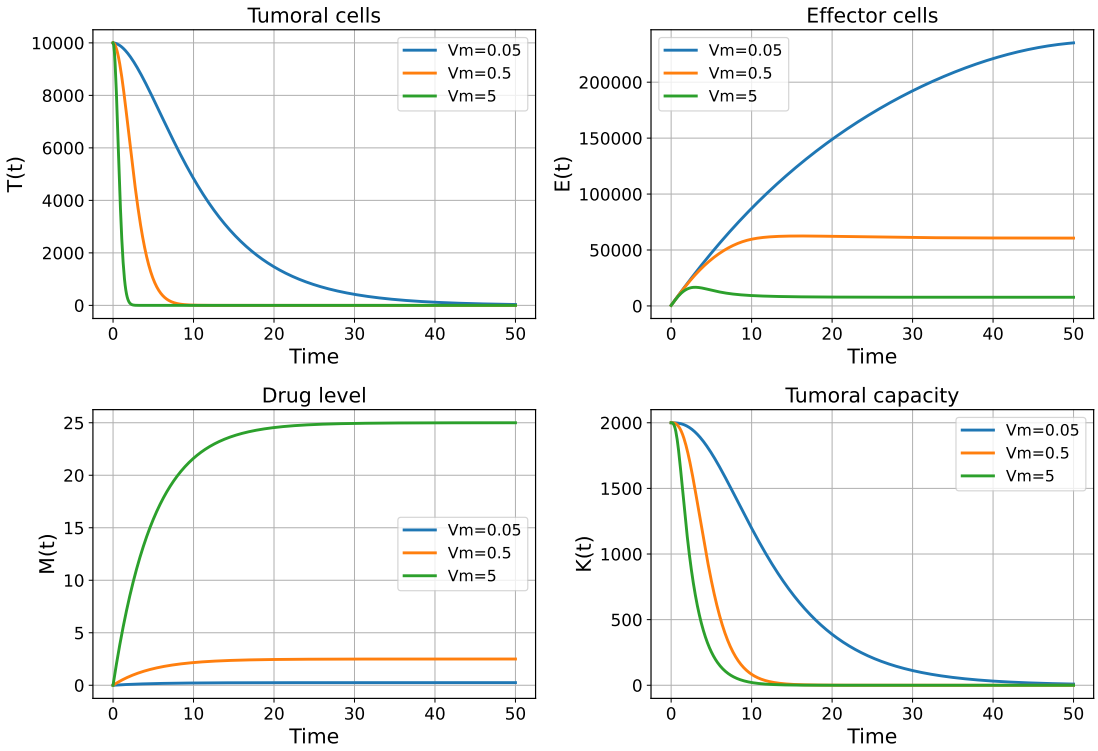

Figure 7. States comparison for different doses of administered medication.

Figure 7 illustrates the model-predicted evolution of the system states under different treatment dosages. For $V_m = 0.05$, the simulated tumor–cell population approaches zero after approximately 30 time units; for $V_m = 0.5$, this occurs after about 10 time units; and for $V_m = 5$, the predicted decline is fastest. Regarding effector immune cells, the simulations show a higher stabilization level with $V_m = 0.05$, which is consistent with a stronger immune activation in response to a larger residual tumor burden, whereas for $V_m = 0.5$, the effector cell population stabilizes at a lower level.

Remark 13. *Within the model, a higher drug dosage V_m is predicted to accelerate tumor decline. We note, however, that the model does not account for treatment toxicity or side effects, so this prediction should not be interpreted as a clinical dosage recommendation without further validation.*

We now compare, within the model, the predicted effects of different therapeutic strategies, including chemotherapy, immunotherapy, anti-angiogenic therapy, and a combination of all three, by varying the corresponding parameters.

Figure 8 illustrates the model-predicted effects of different therapies on tumor cells and their carrying capacity. In the simulations, all four strategies lead to a reduction in tumor cells and carrying capacity; the scenarios corresponding to chemotherapy and to the combination therapy show the fastest predicted tumor decline within this model. Regarding effector immune cells, their simulated population remains comparatively stable, while it increases more markedly under the other two. The administered drug concentration $M(t)$ increases and then stabilizes in the chemotherapy and combination scenarios. In the anti-angiogenic and immunotherapy scenarios, $V_m(t)$ remains close to zero, since in our model formulation these strategies are represented as acting directly on the tumor growth or vascularization terms rather than through the medication input $V_m(t)$.

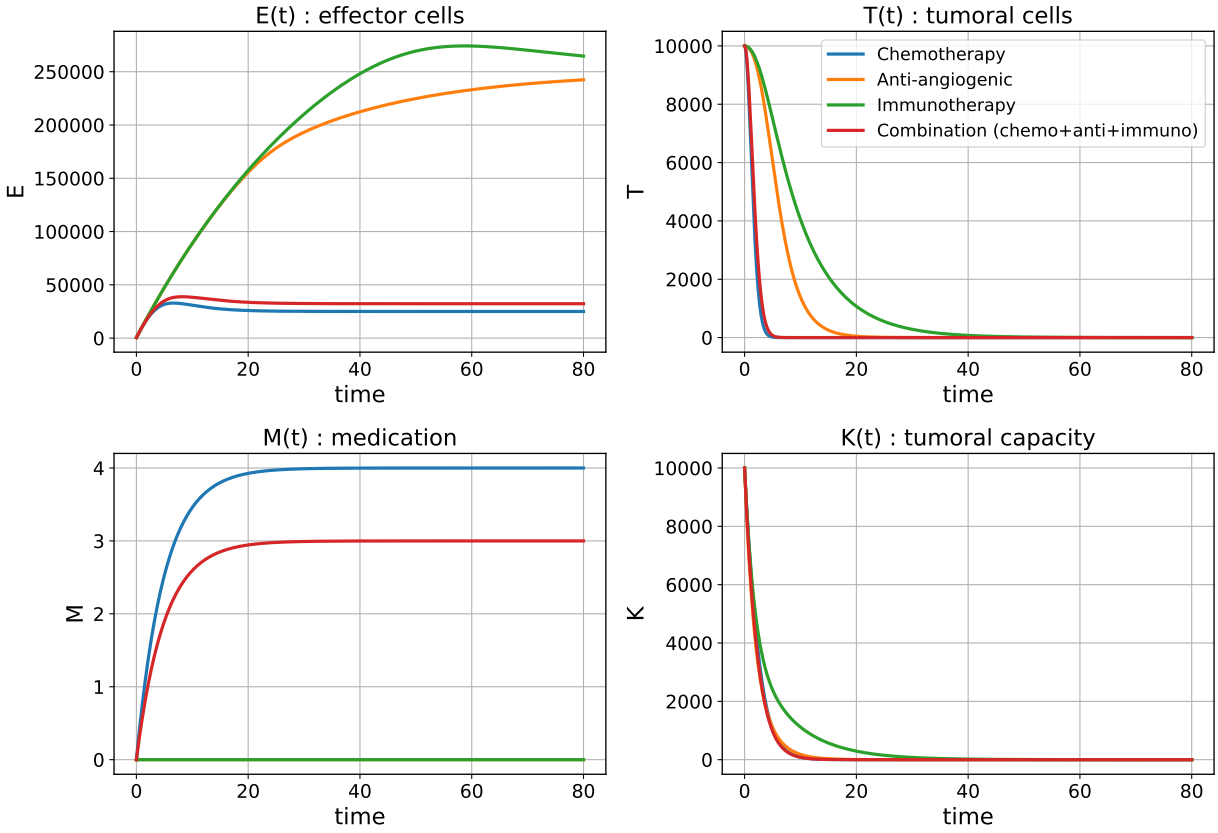

Figure 8. State evolution for different therapies.

6.2. Treatment interruption

In this section, we analyze changes in the different compartments by varying the parameters in each case and interrupting treatment administration at different times.

By analyzing the figures below, we observe the following:

- **Figure 9** illustrates a slow decline in tumor cells and carrying capacity. The tumor nearly disappears around $t = 200$, coinciding with the time of treatment interruption.
- **Figure 10** shows a reduction in tumor cells and carrying capacity until $t = 70$, followed by a resurgence once the treatment is halted.
- **Figure 11** depicts a slight initial decrease in tumor cells, which is quickly followed by a rapid increase after treatment interruption.
- **Figure 12** demonstrates rapid tumor eradication and a sharp decline in carrying capacity due to the high drug dosage.

In all cases, the treatment–administration rate initially remains at its prescribed value and abruptly drops to zero when treatment is interrupted, whereas the treatment concentration subsequently decreases according to its elimination dynamics.

We observe that higher drug dosages lead to faster tumor reduction. However, this approach carries greater risk in real-world scenarios due to potential adverse side effects. A more effective and safer

strategy might involve administering smaller doses over an optimally chosen treatment period; in our case, 200 days.

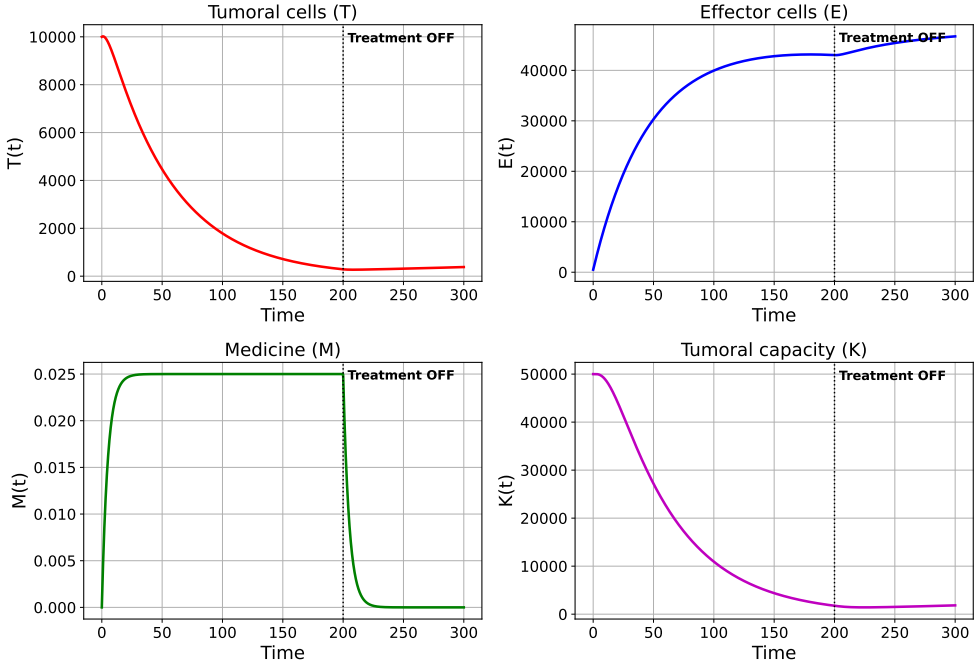

Figure 9. Interruption of treatment at $t = 200$ considering $V_m = 0.005$ and $r = 0.005$.

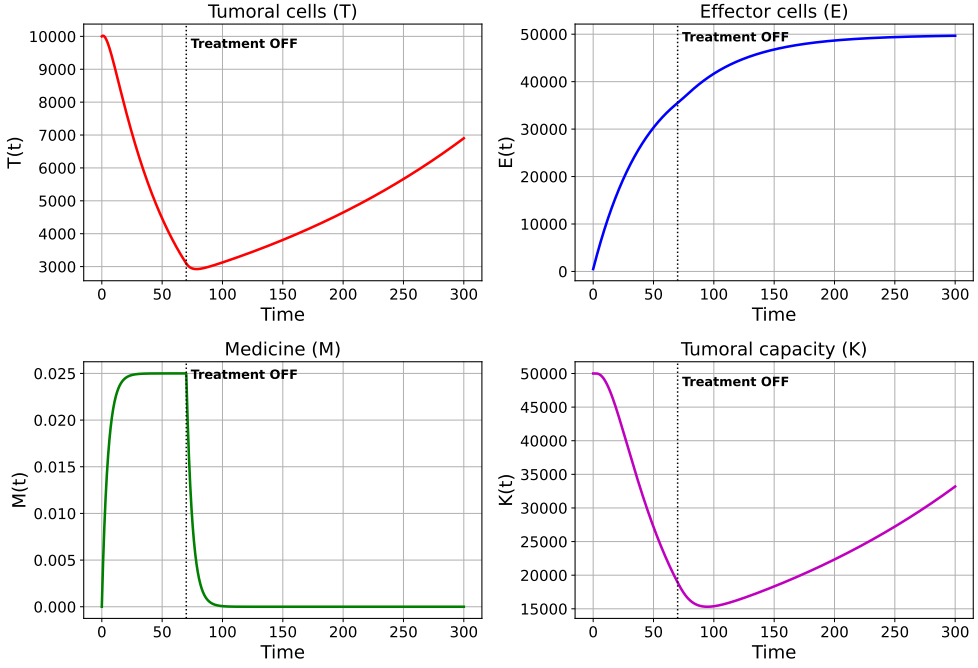

Figure 10. Interruption of the medicine at t=70 considering $V_m = 0.005$ and $r = 0.005$.

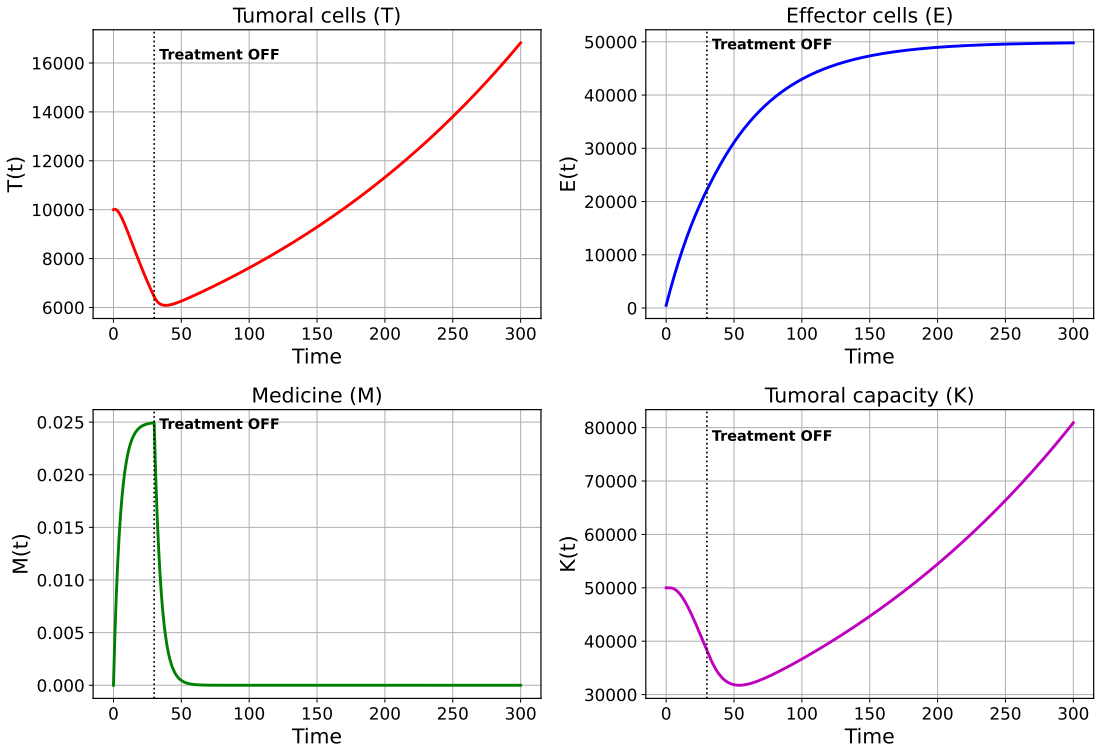

Figure 11. Interruption of the medicine at t=30 considering $V_m = 0.005$ and $r = 0.005$.

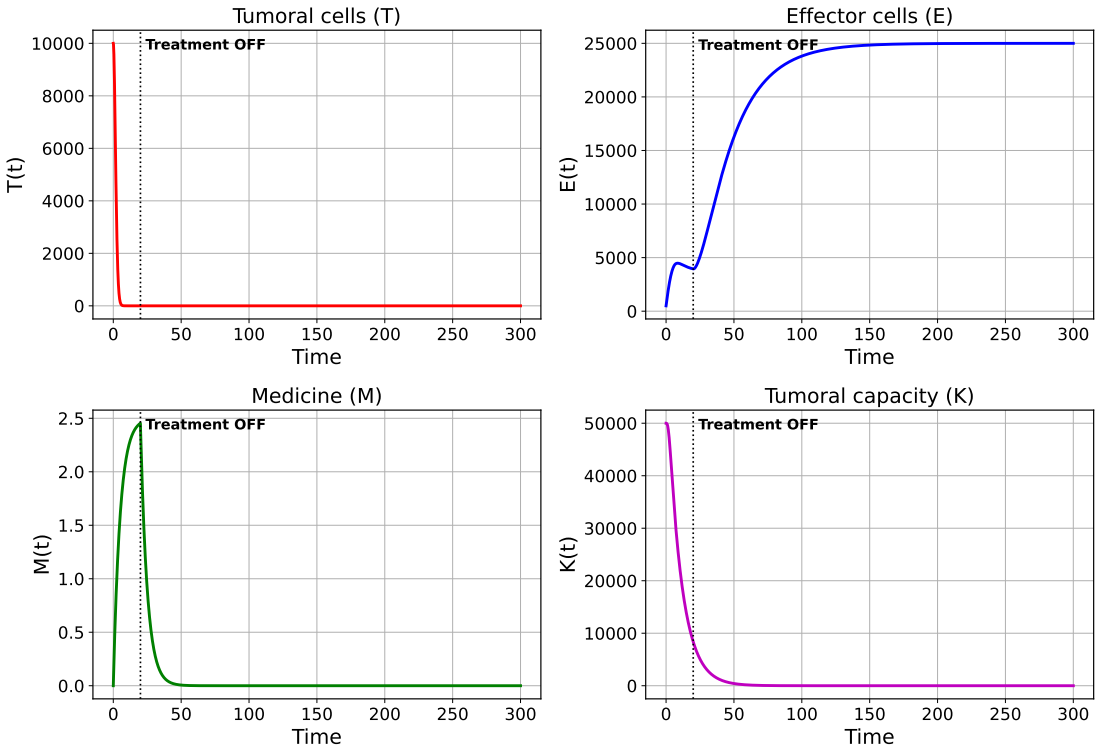

Figure 12. Interruption of the medicine at t=30 considering $V_m = 0.5$ and $r = 0.005$.

We consider three chemotherapy drugs, which differ in the parameters K_E, K_T, and γ. Specifically, we use:

- Chemotherapy A (PCV): $K_T = 0.05$, $K_E = 0.03$, and $\gamma = 0.1$.
- Chemotherapy B (lomustine): $K_T = 0.03$, $K_E = 0.01$, and $\gamma = 0.3$.
- Chemotherapy C (TMZ): $K_T = 0.04$, $K_E = 0.02$, and $\gamma = 0.05$.

Remark 14. *We choose a different final time in this case, to make the differences between the medications clearer.*

Figures 13 and 14 show that, for $t = 50$ and $t = 500$, medication C is the most effective. The residual tumor-cell population under chemotherapy A is very small, while a considerable residual tumor-cell population remains for medication B. At $t = 5000$, tumor cells under chemotherapy A grow more than under B. Medication C consistently results in the lowest residual tumor–cell population.

We also observe that lomustine is the slowest-acting drug in terms of tumor eradication, while it produces the highest increase in effector immune cells.

In conclusion, temozolomide (TMZ) appears to be the most effective chemotherapy in terms of the speed of tumor reduction and the minimal residual tumor–cell population over time.

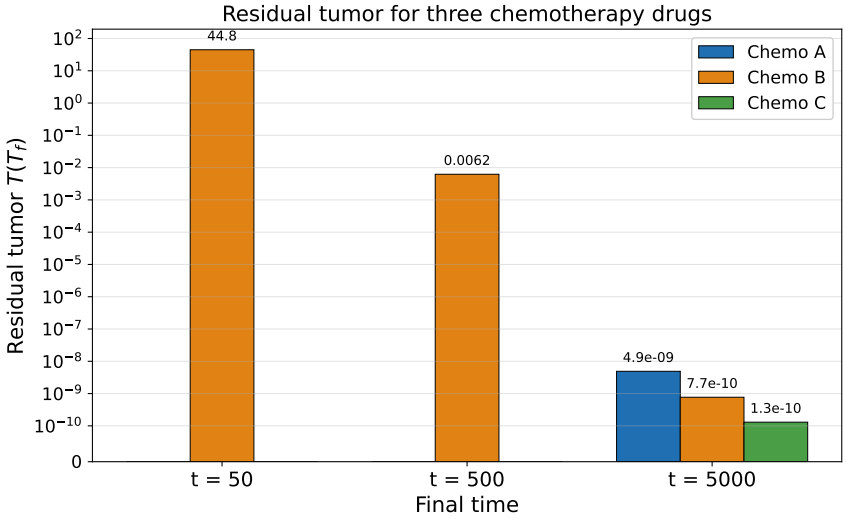

Figure 13. Residual tumor $T(T_f)$ under chemotherapies A, B, and C at $t = 50$, $t = 500$, and $t = 5000$ (logarithmic scale). At $t = 50$ and $t = 500$, the residual tumor under A and C is below the plotted range.

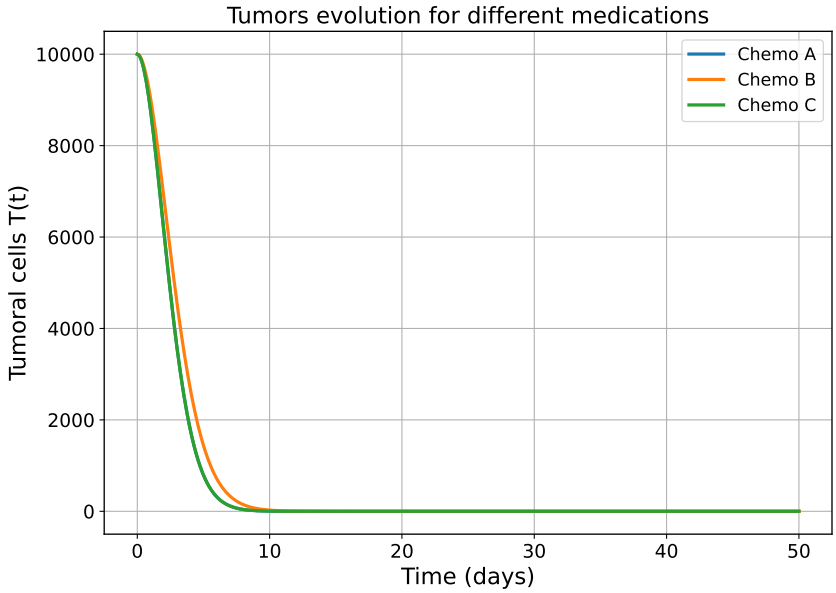

Figure 14. State evolution for different medications.

Remark 15. *The numerical simulations observed in this work are given to illustrate the different properties of the model and the effectiveness of the proposed optimal control strategy. The parameter values are selected from the literature and are chosen to represent biologically plausible scenarios [25, 26]. The numerical results obtained in this work are qualitatively consistent with those reported in the cited works.*

6.3. Comparison with experimental and clinical observations

Provenance of the parameter values. The parameters used above are not chosen arbitrarily. The tumor–immune block of (2.1) is of Kuznetsov–Perelson type, whose coefficients are estimated by Kuznetsov et al. [27] using experimental data on BCL_1 lymphoma in mice, and are reused in the optimal-control study of de Pillis and Radunskaya [28]. The carrying-capacity equation is the linearized form of the vascular-support model of Hahnfeldt et al. [24], calibrated against Lewis lung carcinoma growth data. The parameter ranges are therefore inherited from models already confronted with measurements.

Qualitative agreement with clinical observations. Three features of our simulations may be compared with documented behavior. (i) Our ranking of the three chemotherapies, which identifies temozolomide as the most effective in terms of residual burden, is consistent with the randomized trial of Stupp et al. [29] in glioblastoma. (ii) The regrowth observed when therapy is interrupted too early (Figures 10 and 11), and its absence after a sufficiently long course (Figure 9), are consistent with the clinical rationale for completing adjuvant cycles rather than stopping at radiological response. (iii) The shape of the optimal schedule, an initial interior treatment phase followed by a continuous taper to zero, is closer to observed maximum-tolerated-dose protocols with de-escalation than an abrupt on/off schedule would be.

Limitations. The above is a qualitative consistency check and not a quantitative validation. A genuine validation would require longitudinal, patient-level measurements of tumor volume, effector–

cell counts, and drug concentration for a defined cohort, together with a formal identifiability analysis and parameter estimation with confidence intervals; such data are not available to us. Moreover, there is a structural obstacle specific to this model: The compartment $\mathcal{K}$ represents vascular support and is not a directly observable clinical quantity, and $\mathcal{E}$ is not measured in routine practice either. Fitting the model to the single observable trajectory, the tumor burden, would leave the remaining compartments unidentifiable, and reporting such a fit as a validation against real data would overstate what had been demonstrated. We therefore present the comparison qualitatively and identify confrontation with patient data as the natural continuation of this work.

7. Sensitivity analysis

In this section, we perform a global sensitivity analysis to identify the model parameters that have the greatest impact on disease dynamics. The analysis is based on partial rank correlation coefficients (PRCCs), statistical measures used to quantify the strength and direction of the relationship between a model output and an input parameter, while controlling for the influence of all other parameters.

A p-value is a statistical measure that quantifies the strength of evidence against a null hypothesis. It represents the probability of obtaining results at least as extreme as those observed, under the assumption that the null hypothesis is true. A small p-value indicates that the observed effect is unlikely to have occurred by chance alone, providing evidence to reject the null hypothesis, whereas a large p-value suggests insufficient evidence to reject it.

Following the methodology in [30], we analyze the influence of model parameters on the area under the curve (AUC) of the tumor–cell population T.

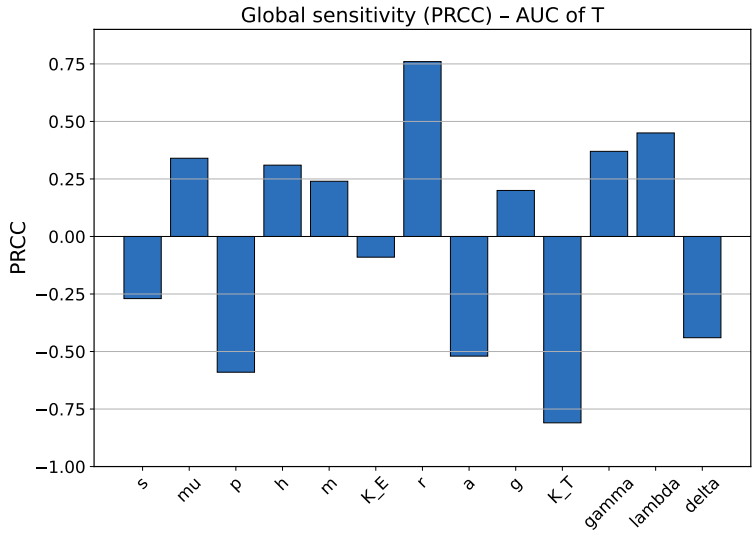

Figure 15. Sensitivity analysis of tumor model using PRCC.

The results presented in Figure 15 and Table 2 indicate that the tumor growth rate r has the strongest positive impact on the tumor AUC, underscoring its central role in driving tumor progression. An increase in r leads to a substantial increase in the cumulative tumor burden over time. Strong negative correlations with tumor AUC are observed for several parameters, suggesting protective or inhibitory

effects on tumor growth. In particular, the immune-related parameters p and a, which regulate immune activation and tumor cell killing, are associated with a marked reduction in tumor burden when their values are increased, highlighting the critical role of immune responses in controlling tumor progression.

Table 2. PRCC-based global sensitivity analysis with respect to the AUC of tumor cells.

Parameter	Interpretation	PRCC	p-value
s	natural growth of normal/effector cells	-0.2682	1.66×10^{-3}
μ	rate of natural demise of effector cells	0.3380	6.08×10^{-5}
p	degree of recruitment of maximum immune-effector cells in relation with cancer cells	-0.5873	7.01×10^{-14}
h	steepness coefficient of the recruitment curve of effector-immune cells	0.3145	2.03×10^{-4}
m	degree of inactivation of effector cells by tumor cells	0.2449	4.20×10^{-3}
$K_{\mathcal{E}}$	drug-induced kill rate of effector cells	-0.0937	2.80×10^{-1}
r	rate of tumor growth	0.7624	6.53×10^{-27}
a	parameter of cancer clean-up	-0.5209	9.40×10^{-11}
g	half-saturation for cancer cleanup	0.1960	2.27×10^{-2}
$K_{\mathcal{T}}$	drug-induced kill rate of tumor cells	-0.8039	8.37×10^{-32}
γ	rate of decrease in concentration of chemotherapy drug	0.3756	7.15×10^{-6}
λ	speed of tumor vascularization	0.4530	3.45×10^{-8}
δ	decay rate of the carrying capacity	-0.4453	6.23×10^{-8}

Remark 16 (Consistency between the sign of the PRCC and the structure of the model)**.** *The strongly negative value* $\mathrm{PRCC}(K_{\mathcal{T}}) = -0.8039$ *is fully consistent with the model once the role of* $K_{\mathcal{T}}$ *is correctly stated. In system* (2.1)*, this parameter multiplies the term* $-K_{\mathcal{T}}\mathcal{M}\mathcal{T}$*, so it measures the* destruction *of tumor cells by the cytotoxic agent; increasing it must therefore decrease the tumor AUC, which is exactly what the negative coefficient expresses.*

Remark 17 (Statistical significance)**.** *Interpreting the magnitude of a PRCC is meaningful only when the associated p-value indicates significance. With a significance level of* 5%*, all parameters in Table 2 are significant except* $K_{\mathcal{E}}$*, for which* $p = 2.80 \times 10^{-1} > 0.05$*. The corresponding coefficient* -0.0937 *is therefore not statistically distinguishable from zero and should not be interpreted as evidence of a protective effect of* $K_{\mathcal{E}}$*; we simply conclude that, over the sampled parameter ranges, the drug-induced loss of effector cells has no detectable monotone influence on the cumulative tumor burden.*

Parameter $K_{\mathcal{T}}$ also exhibits a strong negative PRCC, indicating that therapeutic or immune-mediated mechanisms linked to this parameter significantly limit tumor expansion. As such, $K_{\mathcal{T}}$ emerges as one of the most influential contributors to reducing the overall cumulative tumor burden.

Parameters related to the dynamic carrying capacity, specifically λ and δ, have opposing effects. The production rate λ is positively correlated with tumor AUC, as it enhances the tumor-supporting capacity of the environment, whereas the decay rate δ is negatively correlated, reflecting its role in constraining tumor growth by reducing available resources.

Other parameters, including s, μ, h, m, $K_{\mathcal{E}}$, and γ, exhibit relatively small PRCC magnitudes,

indicating weaker or indirect effects on the tumor AUC. These parameters primarily influence short-term tumor dynamics but have limited impact on cumulative tumor growth over time.

Overall, the PRCC analysis identifies tumor proliferation, immune response efficiency, and regulation of environmental carrying capacity as the dominant mechanisms governing long-term tumor dynamics in this model.

8. Conclusions

In this work, based on a Rosenzweig–MacArthur model, we formulated a framework to study the dynamics of tumor cells and effector immune cells, including the effects of treatment and a time-dependent carrying capacity. For this model, we analyzed the existence, uniqueness, and stability of solutions. We also formulated an optimal control problem, which we solved theoretically and numerically. Different treatments and therapeutic strategies were compared to identify the most appropriate approach in each scenario. Finally, using Partial Rank Correlation Coefficients (PRCC), we performed a global sensitivity analysis to assess the impact of input parameters on tumor dynamics.

We place these results on a firmer footing. Boundedness is now obtained through a total-mass estimate that does not rely on the explicit logistic profile and is therefore valid for a genuinely time-dependent carrying capacity, under the corrected hypothesis $\lambda < \delta$. Existence and uniqueness follow from the continuous differentiability of the vector field on a compact positively invariant region on which the carrying capacity remains bounded away from zero. The existence of the endemic equilibrium is established by an intermediate–value argument, and its local asymptotic stability is now characterized analytically by an explicit Routh–Hurwitz criterion rather than by simulation alone. Finally, the optimal control has been shown to be continuous, taking interior values below the maximum admissible dose and then decreasing continuously to zero, as dictated by the strict convexity of the quadratic cost in the control.

A structural consequence of the corrected analysis deserves emphasis. The endemic equilibrium exists only when $\xi = r(1 - \delta/\lambda) - K_{\mathcal{T}} V_m/\gamma > 0$, hence only when $\lambda > \delta$, which is precisely the regime excluded by the boundedness hypothesis $(H2)$. Tumor persistence at a steady state and boundedness of the solutions are therefore mutually exclusive within this model: When vascular regression dominates neo-vascularization, the only equilibria are the tumor-free states E_0 and E_1. This clarifies the therapeutic message of the model, since maintaining $\lambda < \delta$ eliminates any persistent tumor state, and it explains why no endemic equilibrium could be located numerically for the parameter set used in Section 5.1.

Several directions remain open. The global stability of the tumor-free equilibrium is not addressed here and would require the construction of a suitable Lyapunov function. A variant of the carrying-capacity equation admitting a bounded persistent state, for instance with a saturating vascularization term, would enable the endemic regime to be studied within the bounded setting; this appears to be the most interesting extension. Comparison of the model with longitudinal patient data, together with a formal identifiability and parameter-estimation study, is the natural next step discussed in Subsection 6.3. Finally, extensions incorporating treatment delays, stochastic fluctuations, or spatial heterogeneity of the tumor would broaden the applicability of the framework.

Author contributions

Nacima Moussouni, Louiza Dehbi and Fares Yazid: Conceptualization, Methodology, Formal analysis, Software, Validation, Writing–original draft, Writing–review and editing; Hicham Saber and Abdelkader Moumen: Supervision, Validation, Writing–review and editing; Khaled Aldwoah and Mohamed Bouye: Writing–review and editing. All authors have read and approved the final version of the manuscript.

Use of AI tools declaration

The authors declare they have not used Artificial Intelligence (AI) tools in the creation of this research.

Acknowledgment

The authors extend their appreciation to the Deanship of Research and Graduate Studies at King Khalid University for funding this work through Large group research project under grant number RGP2/559/47.

Conflict of interest

The authors declare no conflicts of interest.

References

1. L. Pecorino, *Molecular biology of cancer: mechanisms, targets, and therapeutics*, 5 Eds., Oxford University Press, 2021.
2. R. A. Weinberg, *The biology of cancer*, New York: W. W. Norton & Company, 2006. https://doi.org/10.1201/9780203852569
3. P. Essunger, A. S. Perelson, Modeling HIV infection of $CD4^+$ T-cell subpopulations, *J. Theor. Biol.*, **170** (1994), 367–391. http://doi.org/10.1006/jtbi.1994.1199
4. H. Moore, N. K. Li, A mathematical model for chronic myelogenous leukemia (CML) and T-cell interaction, *J. Theor. Biol.*, **227** (2004), 513–523. http://doi.org/10.1016/j.jtbi.2003.11.024
5. A. M. D. Clotilda, G. V. R. K. Vithanage, D. D. Lakshika, A mathematical model for cancer treatment using chemotherapy and immunotherapy under mass-action kinetics, *Molecular Sciences and Applications*, **4** (2024), 150–161. http://doi.org/10.37394/232023.2024.4.15
6. D. Lestari, E. R. Sari, H. Arifah, Dynamics of a mathematical model of cancer cells with chemotherapy, *J. Phys.: Conf. Ser.*, **1320** (2019), 012026. http://doi.org/10.1088/1742-6596/1320/1/012026
7. A. J. Lotka, *Elements of physical biology*, Baltimore: Williams & Wilkins, 1925.
8. V. Volterra, Fluctuations in the abundance of a species considered mathematically, *Nature*, **118** (1926), 558–560. https://doi.org/10.1038/118558a0

9. H. Deng, F. Chen, Z. Zhu, Z. Li, Dynamic behaviors of a Lotka–Volterra predator–prey model incorporating predator cannibalism, *Adv. Differ. Equ.*, **2019** (2019), 359. http://doi.org/10.1186/s13662-019-2289-8

10. M. Swailem, U. C. Täuber, Lotka–Volterra predator–prey model with periodically varying carrying capacity, *Phys. Rev. E*, **107** (2023), 064144. http://doi.org/10.1103/PhysRevE.107.064144

11. N. O. Nweze, N. M. Offiong, M. U. Adehi, S. E. Chaku, S. Abdullahi, Modeling of species interaction in a habitat using Lotka–Volterra type systems, *IOSR Journal of Mathematics*, **10** (2014), 45–54. http://doi.org/10.9790/5728-10444554

12. M. J. Uddin, M. M. Khan, I. M. Alsulami, A. Alsulami, Complex dynamics of a discretized Rosenzweig–MacArthur prey–predator model with fear effect and prey refuge, *AIMS Math.*, **10** (2025), 14629–14656. http://doi.org/10.3934/math.2025659

13. B. Xie, Impact of fear and Allee effect on a Holling type II prey–predator model, *Adv. Differ. Equ.*, **2021** (2021), 464. http://doi.org/10.1186/s13662-021-03592-6

14. M. W. Yasin, N. Ahmed, J. Saeed, A. Raza, M. Rafiq, H. Ahmad, et al., Numerical study of a reaction–diffusion prey–predator model with Holling II functional response under noisy environment, *J. Nonlinear Math. Phys.*, **31** (2024), 68. http://doi.org/10.1007/s44198-024-00238-5

15. J. Wang, L. Pan, Qualitative analysis of a harvested predator–prey system with Holling type III functional response incorporating prey refuge, *Adv. Differ. Equ.*, **2012** (2012), 96. http://doi.org/10.1186/1687-1847-2012-96

16. Q. Jiang, J. Wang, Qualitative analysis of a harvested predator–prey system with Holling type III functional response, *Adv. Differ. Equ.*, **2013** (2013), 249. http://doi.org/10.1186/1687-1847-2013-249

17. F. Munteanu, Jacobi stability of the Rosenzweig–MacArthur predator–prey system via KCC geometric theory, *Symmetry*, **14** (2022), 1815. http://doi.org/10.3390/sym14091815

18. L. Pontryagin, *Mathematical theory of optimal processes*, London: Routledge, 1987. http://doi.org/10.1201/9780203749319

19. N. Moussouni, M. Aliane, L. Dehbi, Optimal control: prey and predator optimization in two- and three-species cases, *Int. J. Dyn. Control*, **13** (2025), 228. http://doi.org/10.1007/s40435-025-01729-z

20. A. J. Abougarair, M. Bakouri, A. Alduraywish, O. G. Mrehel, A. Alqahtani, T. Alqahtani, et al., Optimizing cancer treatment using optimal control theory, *AIMS Math.*, **9** (2024), 31740–31769. http://doi.org/10.3934/math.20241526

21. A. Das, K. Dehingia, H. K. Sharmah, C. Park, J. R. Lee, K. Sadri, et al., Optimal control of effector–tumor–normal cell dynamics in the presence of adoptive immunotherapy, *AIMS Math.*, **6** (2021), 9813–9834. http://doi.org/10.3934/math.2021570

22. L. Huang, J. Wang, J. Li, T. Ma, Analysis of rumor spreading with different usage ranges in a multilingual environment, *AIMS Math.*, **9** (2024), 24018–24038. http://doi.org/10.3934/math.20241168

23. K. Zhang, Y. Ji, Q. Pan, Y. Wei, Y. Ye, H. Liu, Sensitivity analysis and optimal treatment control for a mathematical model of human papillomavirus infection, *AIMS Math.*, **5** (2020), 2646–2670. http://doi.org/10.3934/math.2020172

24. P. Hahnfeldt, D. Panigrahy, J. Folkman, L. Hlatky, Tumor development under angiogenic signaling: a dynamical theory of tumor growth, treatment response, and postvascular dormancy, *Cancer Res.*, **59** (1999), 4770–4775.

25. N. G. Laleh, C. M. L. Loeffler, J. Grajek, K. Stanková, A. T. Pearson, H. S. Muti, et al., Classical mathematical models for prediction of response to chemotherapy and immunotherapy, *PLoS Comput. Biol.*, **18** (2022), e1009822. http://doi.org/10.1371/journal.pcbi.1009822

26. G. Lorenzo, D. A. Hormuth II, C. Wu, G. Pash, A. Chaudhuri, E. A. B. F. Lima, et al., Validating the predictions of mathematical models describing tumor growth and treatment response, arXiv:2502.19333. http://doi.org/10.48550/arXiv.2502.19333

27. V. A. Kuznetsov, I. A. Makalkin, M. A. Taylor, A. S. Perelson, Nonlinear dynamics of immunogenic tumors: parameter estimation and global bifurcation analysis, *Bull. Math. Biol.*, **56** (1994), 295–321. http://doi.org/10.1016/S0092-8240(05)80260-5

28. L. G. de Pillis, A. Radunskaya, The dynamics of an optimally controlled tumor model: a case study, *Math. Comput. Model.*, **37** (2003), 1221–1244. http://doi.org/10.1016/S0895-7177(03)00133-X

29. R. Stupp, W. P. Mason, M. J. van den Bent, M. Weller, B. Fisher, M. J.B. Taphoorn, et al., Radiotherapy plus concomitant and adjuvant temozolomide for glioblastoma, *New Engl. J. Med.*, **352** (2005), 987–996. http://doi.org/10.1056/NEJMoa043330

30. S. Marino, I. B. Hogue, C. J. Ray, D. E. Kirschner, A methodology for performing global uncertainty and sensitivity analysis in systems biology, *J. Theor. Biol.*, **254** (2008), 178–196. http://doi.org/10.1016/j.jtbi.2008.04.011

AIMS Press